



US009297693B2

(12) **United States Patent**
Furxhi et al.

(10) **Patent No.:** **US 9,297,693 B2**
(45) **Date of Patent:** **Mar. 29, 2016**

(54) **SPATIALLY-SELECTIVE REFLECTOR STRUCTURES, REFLECTOR DISKS, AND SYSTEMS AND METHODS FOR USE THEREOF**

(71) Applicant: **The University of Memphis Research Foundation**, Memphis, TN (US)

(72) Inventors: **Orges Furxhi**, Durham, NC (US); **Eddie L. Jacobs**, Memphis, TN (US); **Thomas Layton**, Memphis, TN (US)

(73) Assignee: **The University of Memphis Research Foundation**, Memphis, TN (US)

(*) Notice: Subject to any disclaimer, the term of this patent is extended or adjusted under 35 U.S.C. 154(b) by 280 days.

(21) Appl. No.: **13/963,528**

(22) Filed: **Aug. 9, 2013**

(65) **Prior Publication Data**

US 2013/0321642 A1 Dec. 5, 2013

Related U.S. Application Data

(63) Continuation of application No. 12/713,049, filed on Feb. 25, 2010, now Pat. No. 8,508,592.

(60) Provisional application No. 61/155,316, filed on Feb. 25, 2009, provisional application No. 61/301,433, filed on Feb. 4, 2010.

(51) **Int. Cl.**

H04N 7/18 (2006.01)

G01J 1/04 (2006.01)

(Continued)

(52) **U.S. Cl.**

CPC . **G01J 1/04** (2013.01); **G01V 8/005** (2013.01);
G02B 26/0816 (2013.01); **H04N 5/33**
(2013.01); **G06K 9/78** (2013.01); **Y10T**
29/49888 (2015.01); **Y10T 156/10** (2015.01)

(58) **Field of Classification Search**

CPC **G06K 9/78**

USPC **348/143**

See application file for complete search history.

(56) **References Cited**

U.S. PATENT DOCUMENTS

2,880,355 A 3/1959 Epsztein

4,019,053 A 4/1977 Levine

(Continued)

FOREIGN PATENT DOCUMENTS

JP 2008-241352 10/2008

OTHER PUBLICATIONS

“Camera ‘looks’ through clothing” <http://newsvote.bbc.co.uk/mpappa/pagetools/print/ners.bbc.co.uk/1/h...> (2008).

(Continued)

Primary Examiner — Glenford Madamba

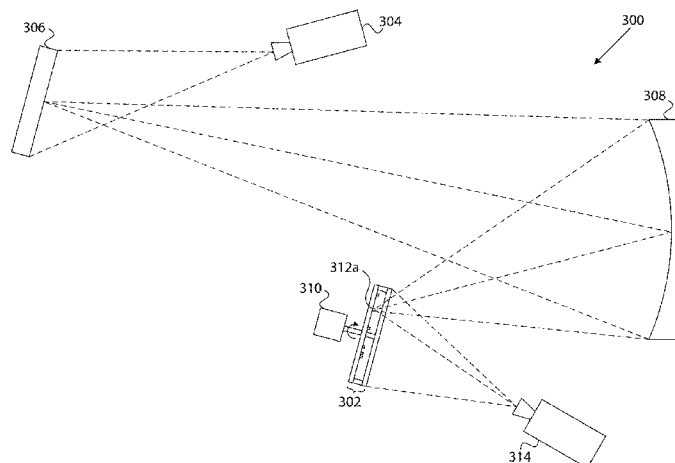
(74) *Attorney, Agent, or Firm* — Mintz Levin Cohn Ferris Glovsky and Popeo, P.C.; Peter F. Corless; Carolina E. Săve

(57)

ABSTRACT

The invention provides a spatially-selective reflective structure for the detection of submillimeter electromagnetic waves and systems and methods incorporating spatially-selective reflective structures. One aspect of the invention provides a spatially-selective reflective structure including a partially-conducting slab and a modulating reflector disk adjacent to the partially-conducting slab. The modulating reflector disk includes a plurality of modulations. Another aspect of the invention provides a submillimeter imaging device including submillimeter wave optics, a spatially-selective reflective structure located in the focal plane of the submillimeter wave optics, a submillimeter wave receiver positioned to capture waves reflected from the spatially-selective reflective structure, and a motor configured to rotate the spatially-selective reflective structure. The spatially-selective reflective structure includes a partially-conducting slab and a modulating reflector disk adjacent to the partially-conducting slab. The modulating reflector plate includes one or more modulations.

3 Claims, 31 Drawing Sheets



(51) **Int. Cl.**
G01V 8/00
G02B 26/08
H04N 5/33
G06K 9/78

(2006.01)
(2006.01)
(2006.01)
(2006.01)

(56)

References Cited

U.S. PATENT DOCUMENTS

4,531,076	A	7/1985	Holder
4,802,748	A	2/1989	McCarthy
4,917,478	A	4/1990	Petran et al.
5,067,805	A	11/1991	Corle et al.
5,202,692	A	4/1993	Huguenin et al.
5,587,832	A	12/1996	Krause
5,642,394	A	6/1997	Rothschild
5,663,639	A	9/1997	Brown
5,666,441	A	9/1997	Rao et al.
5,789,750	A	8/1998	Nuss
5,867,251	A	2/1999	Webb
5,923,466	A	7/1999	Krause et al.
6,144,679	A	11/2000	Herman et al.
6,242,740	B1 *	6/2001	Luukanen et al. 250/353
6,359,582	B1	3/2002	MacAleese et al.
6,469,624	B1	10/2002	Whan et al.
6,587,246	B1	7/2003	Anderton et al.
6,815,683	B2	11/2004	Federick et al.
6,816,647	B1	11/2004	Rudd
7,105,820	B2	9/2006	Federici et al.
7,113,534	B2	9/2006	Unterrainer et al.
7,152,007	B2	12/2006	Arnone et al.
7,174,037	B2	2/2007	Arnone et al.
7,310,442	B2	12/2007	Monachino et al.
7,326,930	B2	2/2008	Crawely
7,342,230	B2	3/2008	Adamski
7,345,279	B2	3/2008	Mueller
7,359,418	B2	4/2008	Edamura et al.
7,386,024	B2	6/2008	Sekiguchi et al.
7,417,440	B2	8/2008	Peschmann et al.
7,439,511	B2	10/2008	Demers
7,449,695	B2	11/2008	Zimdars
2004/0022436	A1	2/2004	Patti et al.
2004/0065831	A1	4/2004	Federici et al.
2005/0058242	A1	3/2005	Peschmann
2005/0117700	A1	6/2005	Peschmann
2005/0156110	A1	7/2005	Crawely
2005/0242287	A1	11/2005	Hakimi
2006/0054824	A1	3/2006	Federici et al.
2006/0214107	A1	9/2006	Mueller
2006/0257005	A1	11/2006	Bergeron et al.
2006/0273255	A1 *	12/2006	Volkov et al. 250/336.1
2007/0058037	A1	3/2007	Bergeron et al.
2007/0228280	A1	10/2007	Mueller
2007/0229937	A1	10/2007	Josef Moeller
2007/0235652	A1	10/2007	Smith
2007/0257194	A1	11/2007	Mueller

2007/0263226	A1	11/2007	Kurtz et al.
2008/0002744	A1	1/2008	Korenblit
2008/0062262	A1	3/2008	Perron et al.
2008/0069164	A1	3/2008	Edamura et al.
2008/0159342	A1	7/2008	McCaughan
2008/0179527	A1	7/2008	Demers
2008/0211713	A1	9/2008	Jeck
2008/0212742	A1	9/2008	Hughes
2008/0217536	A1	9/2008	Sekiguchi
2008/0219308	A1	9/2008	Yamanishi et al.
2009/0140961	A1	6/2009	Geisow et al.
2009/0246707	A1	10/2009	Li et al.

OTHER PUBLICATIONS

"From the lab to the Shop Floor," http://picometric.com/pico_products/terahertz_tr4000.asp, (2008).

Harold Jacobs, "A Bulk Semiconductor Imaging Device for Millimeter and Submillimeter Radiation," Edition 16, Volume No. 5, pp. 419-424 (1969).

Matthews et al., "Vector Markup Language (VML)", <http://www.w3.org/TR/NOTE-VML>, (1998).

Slamani et al., "Image Processing Tools for the Enhancement of Concealed Weapon Detection," IEEE, pp. 518-522 (1999).

Picometrix, "T-Ray 2000: Research Application Development," http://picomeric.com/pico_products/terahertz_research.asp (2008).

Coherent, "SIFIR-50" (2007).

Picometrix, "T-Ray 4000: From the Lab to the Shop Floor," http://picometric.com/pico_products/terahertz_tr4000.asp (2008).

ThruVision, Press Release, "TruVision Introduces T5000 Security Imaging System to 'see' concealed items under clothing at extended ranges outdoors," (2008).

W3C, Scalable Vector Graphics (SVG), <http://www.w3.org/Graphics/SVG/> (2010).

"Thruvision—T5000," <http://www.thruvision.com/t5000.html> (2008).

David K. Cheng, "Field and Wave Electromagnetics" The Addison-Wesley series in Electrical Engineering, pp. 388-398 (1989).

Barbirato et al., "Fracarro, from the Disk of Nipkow to the Digital Convergence," in HISTELCON-08 96-101 (2008).

Chris Tillery, "Detecting Concealed Weapons: Directions for the Future," 258 NIJ Journal 26-28 (2007).

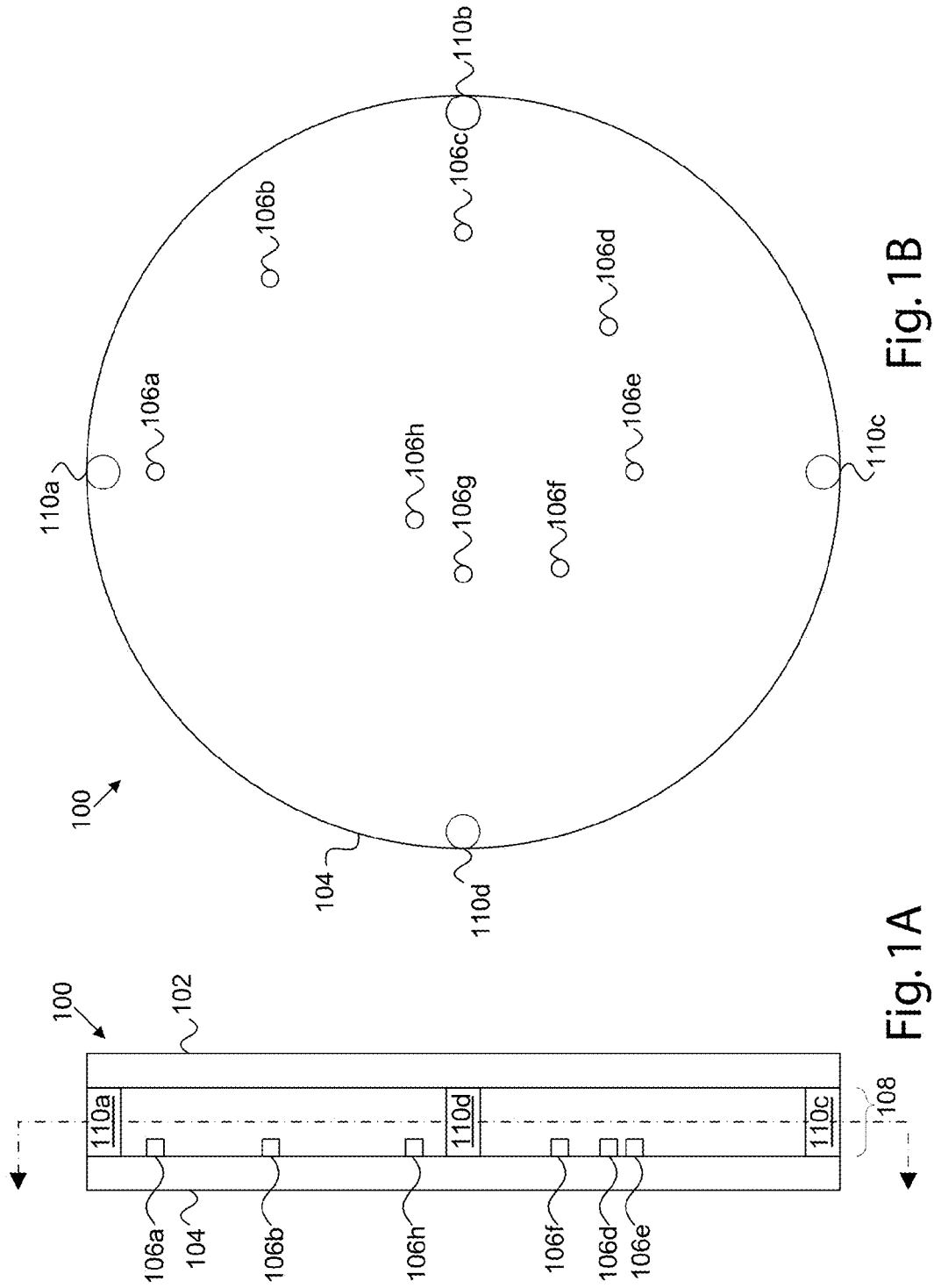
Furxhi et al. "Analysis of a device for single pixel terahertz imaging," 6949 Proc. SPIE (2008).

Furxhi et al. "Design and analysis of a spatially selective mirror for submillimeter-wave imaging," 7309 Proc. SPIE (2009).

International Search Report for International Application No. PCT/US2010/025426, dated Aug. 20, 2010.

Written Opinion for International Application No. PCT/US2010/025426, dated Aug. 20, 2010.

* cited by examiner



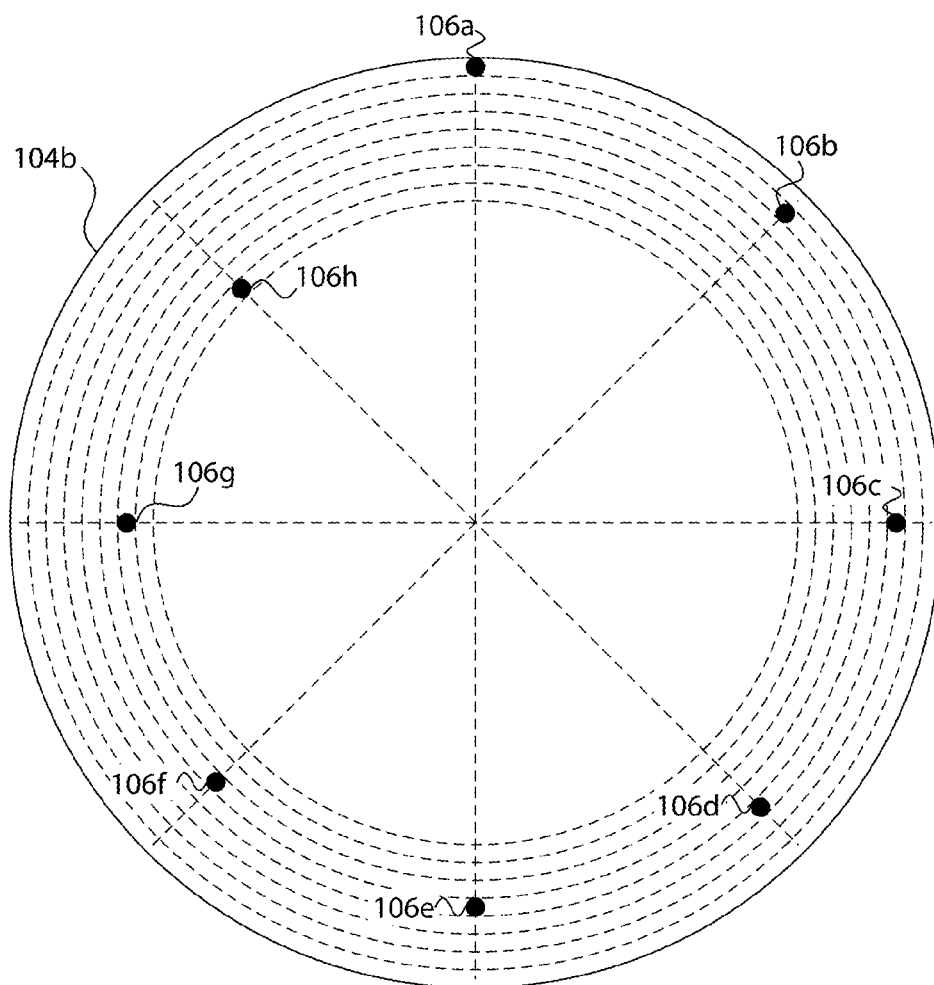


Fig. 1C

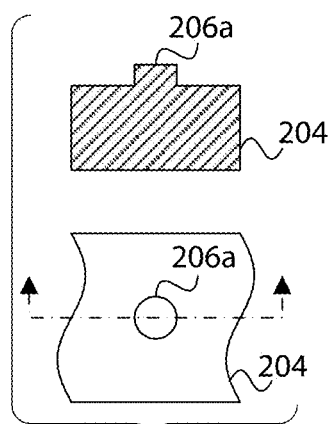


Fig. 2A

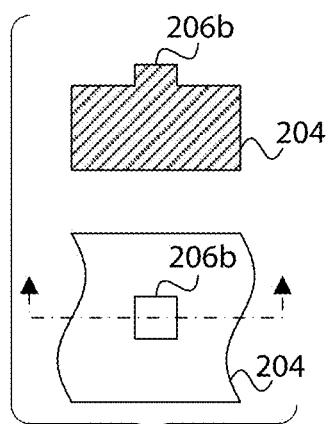


Fig. 2B

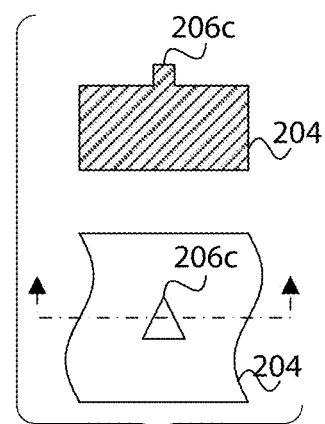


Fig. 2C

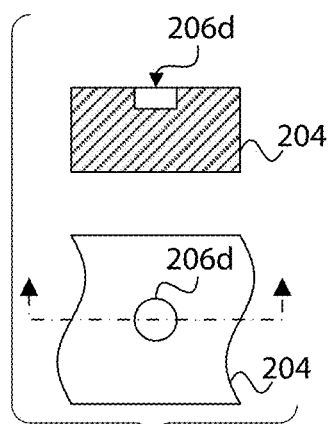


Fig. 2D

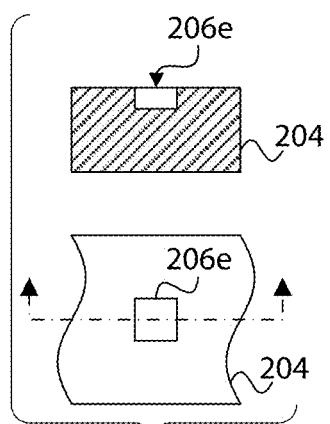


Fig. 2E

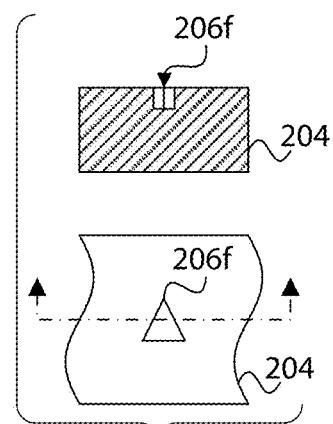


Fig. 2F

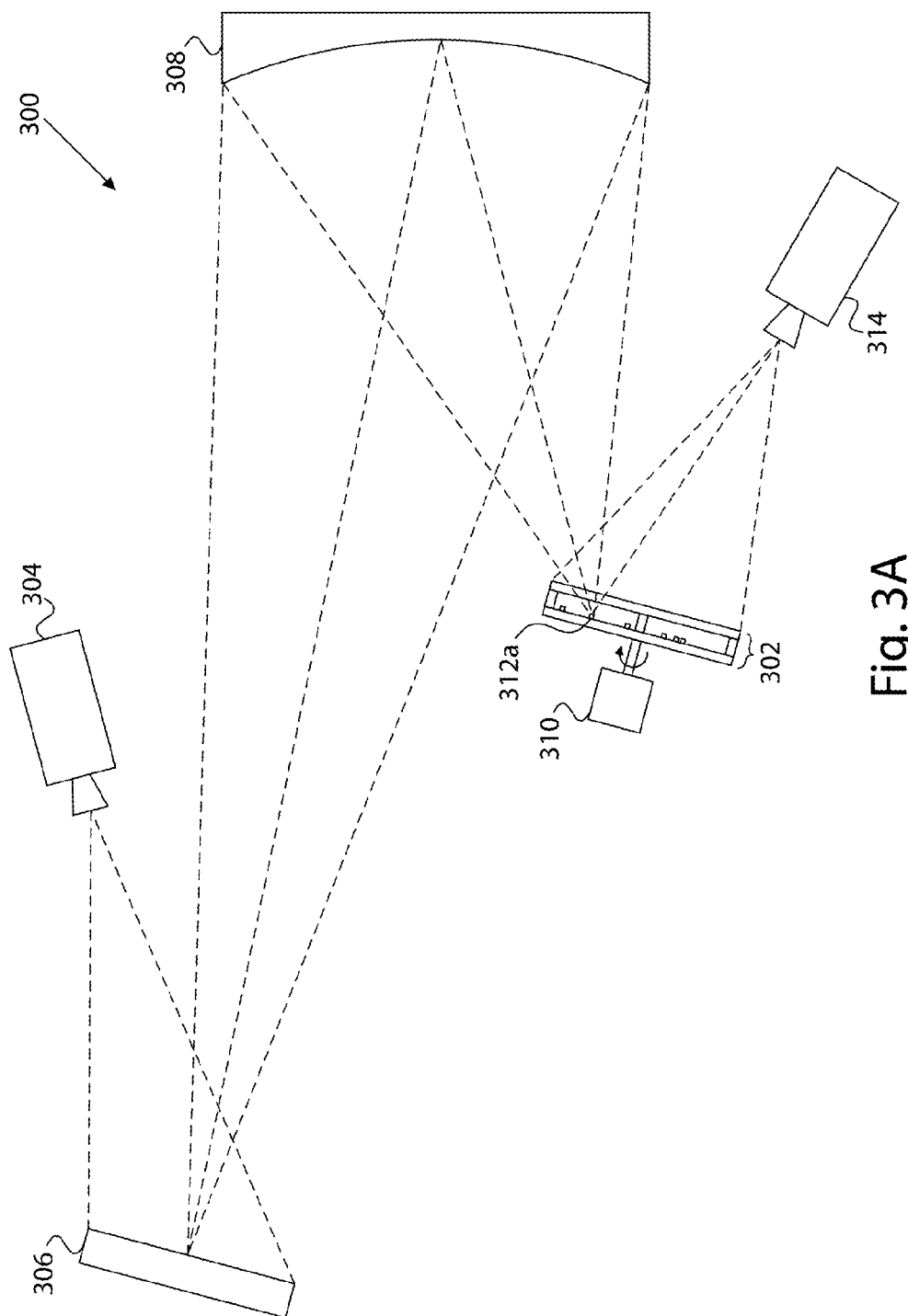


Fig. 3A

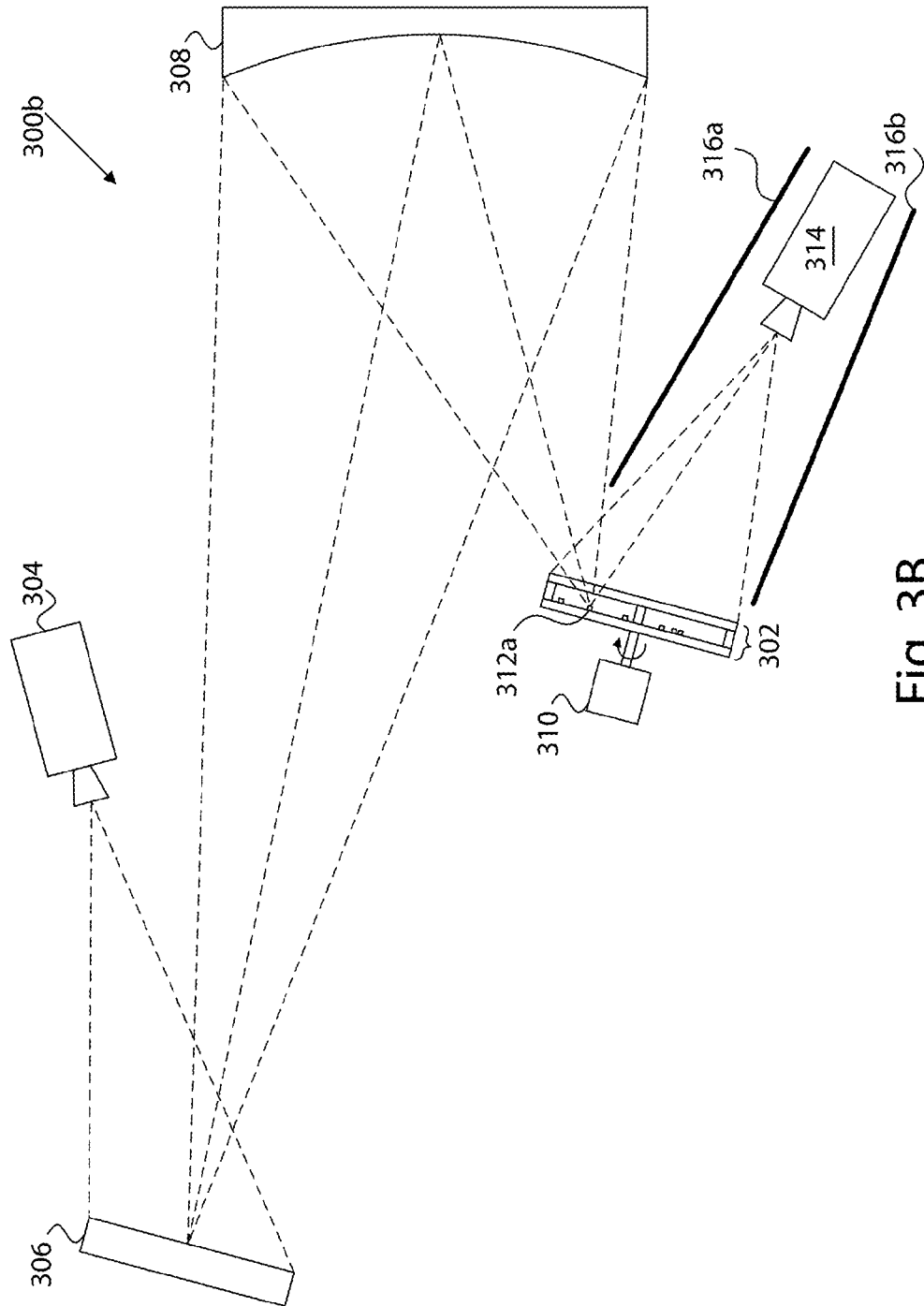


Fig. 3B

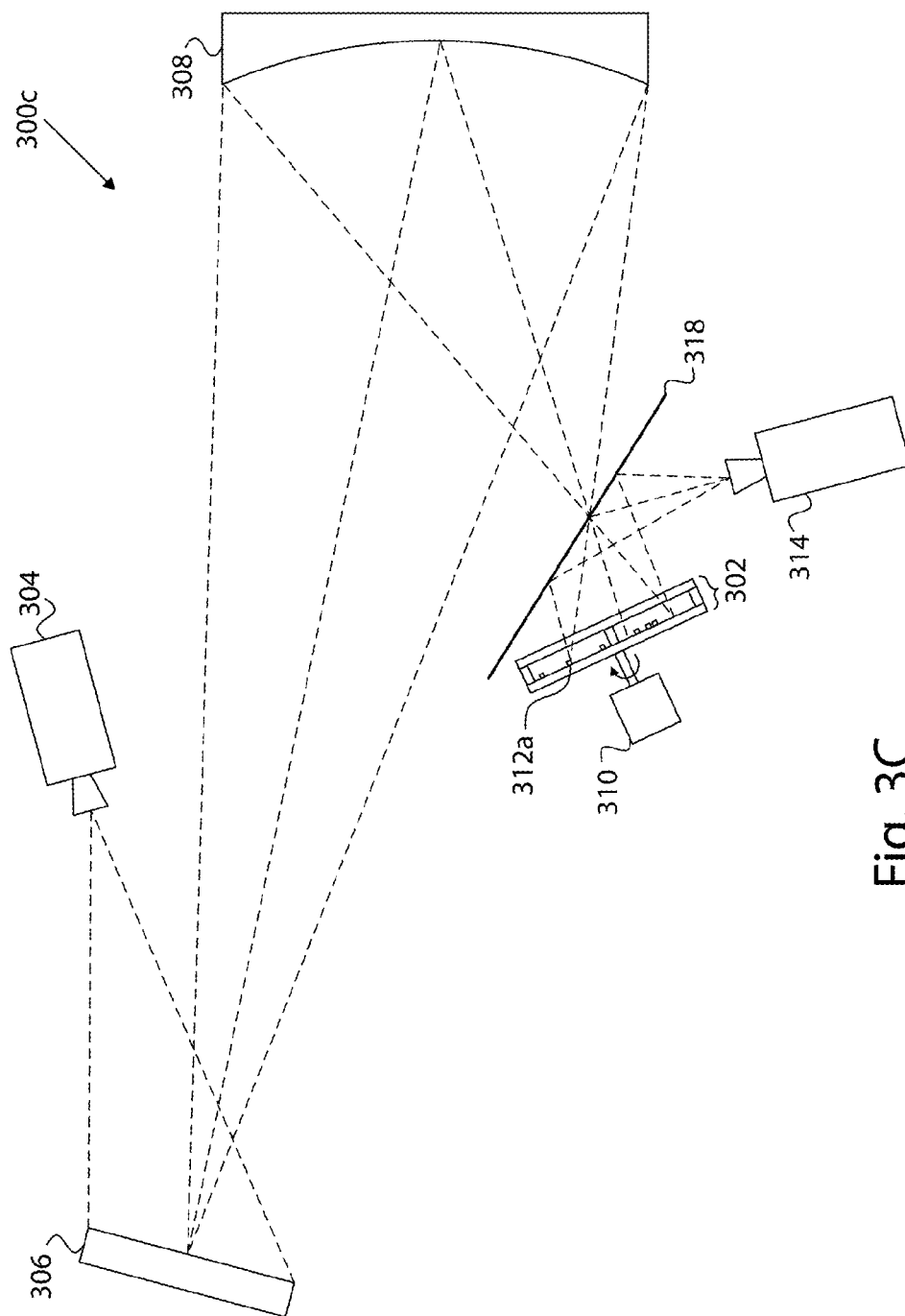


Fig. 3C

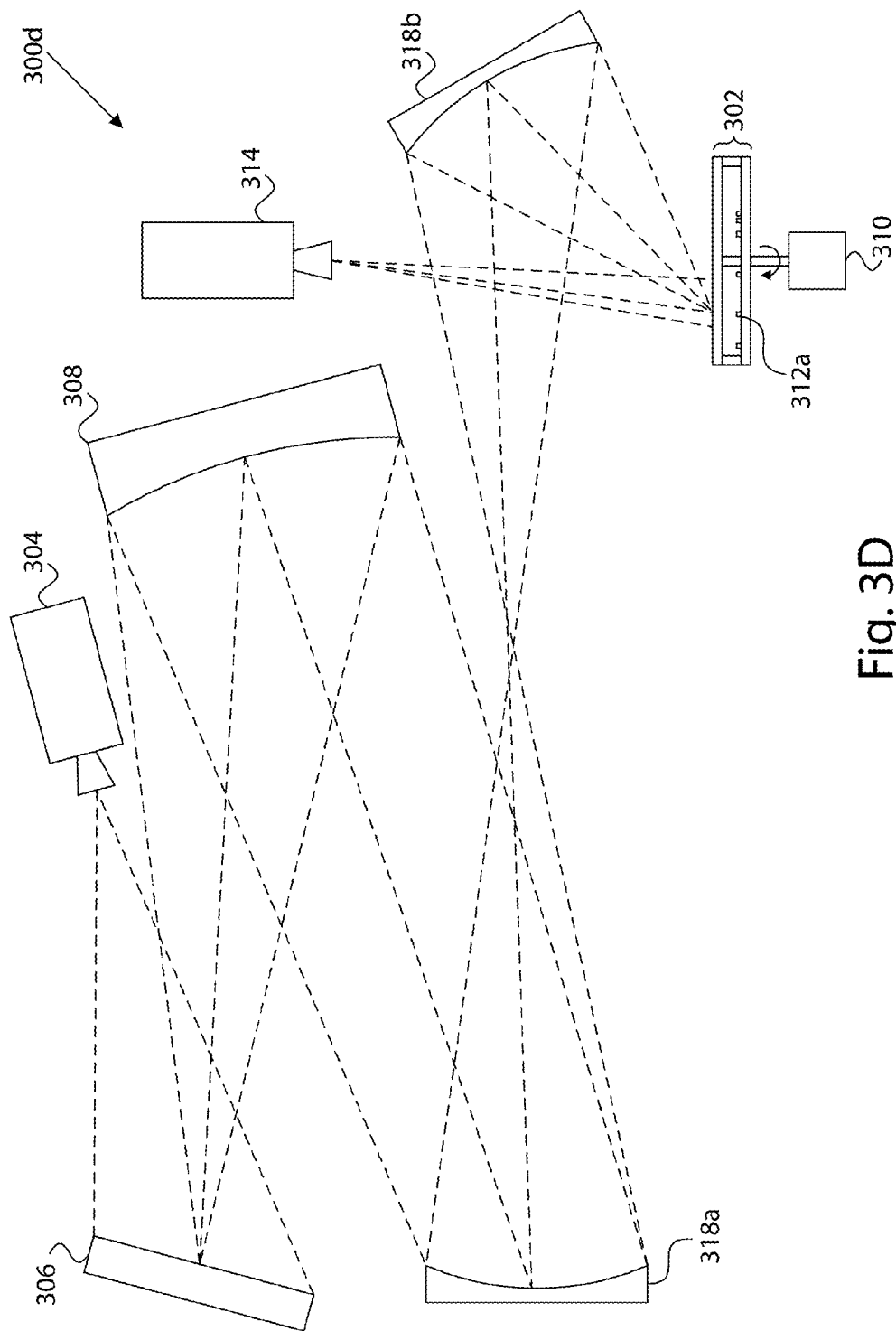


Fig. 3D

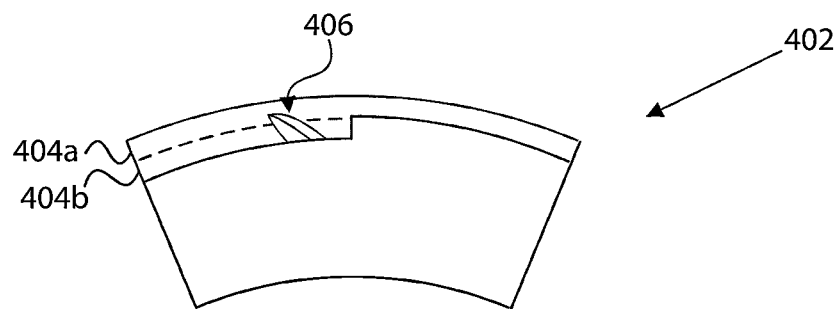


Fig. 4A

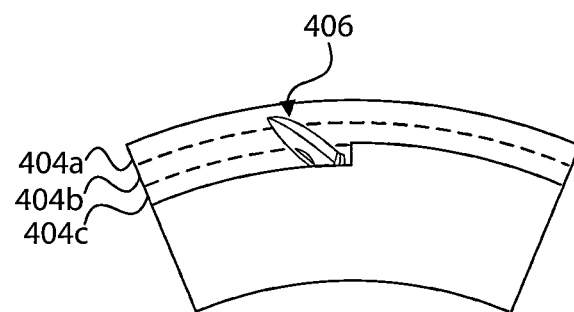


Fig. 4B

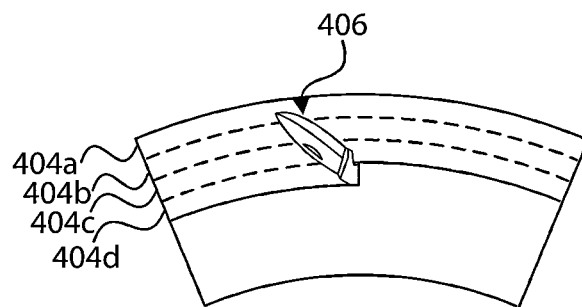


Fig. 4C

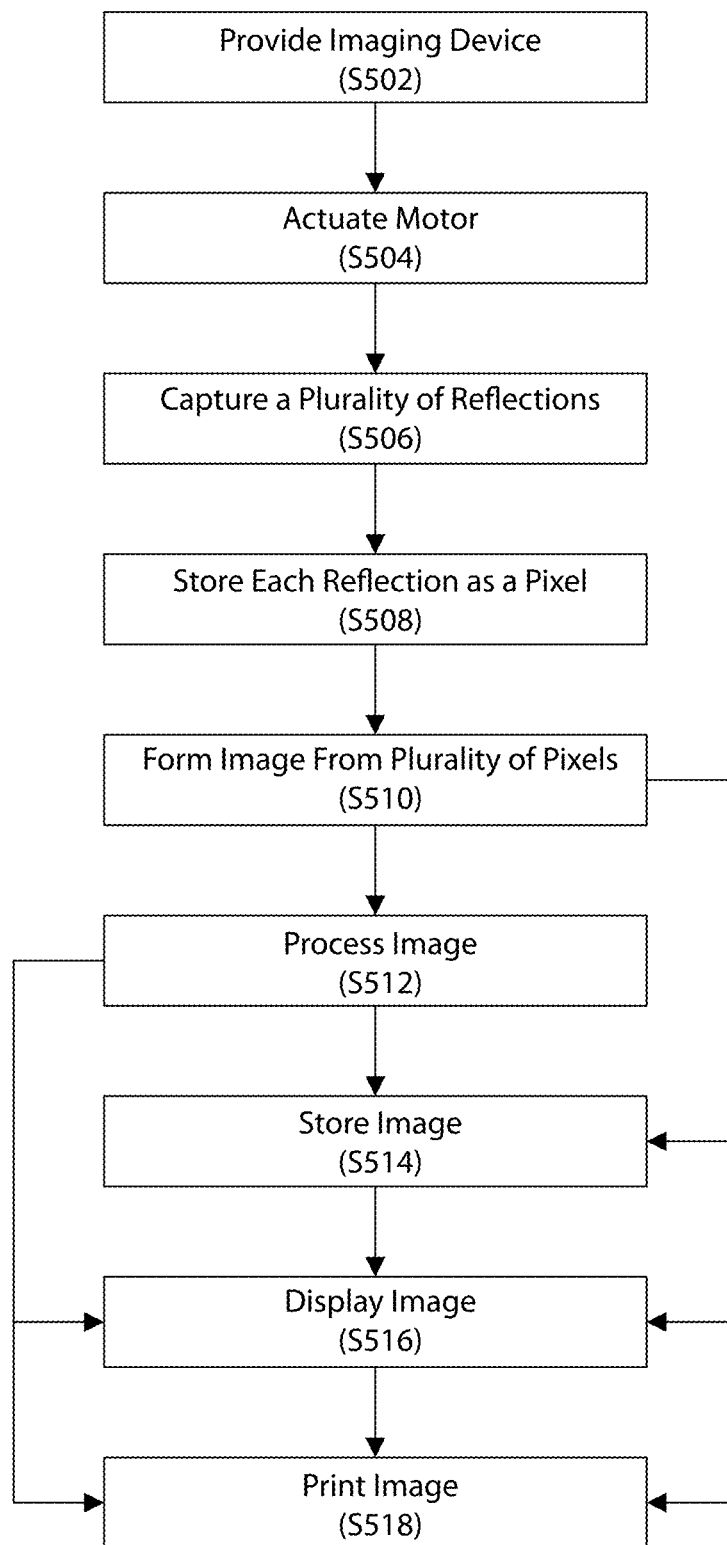


Fig. 5

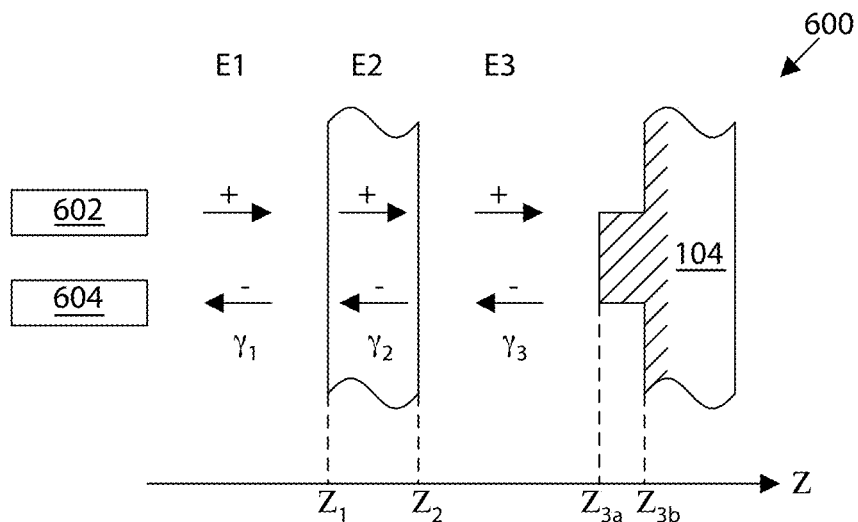


Fig. 6A

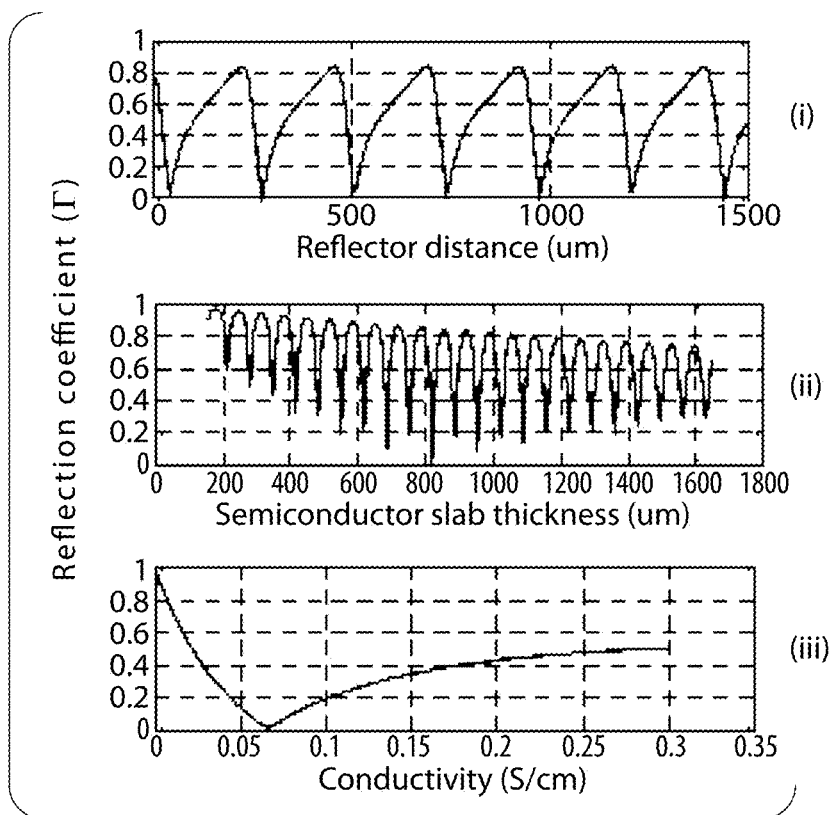


Fig. 6B

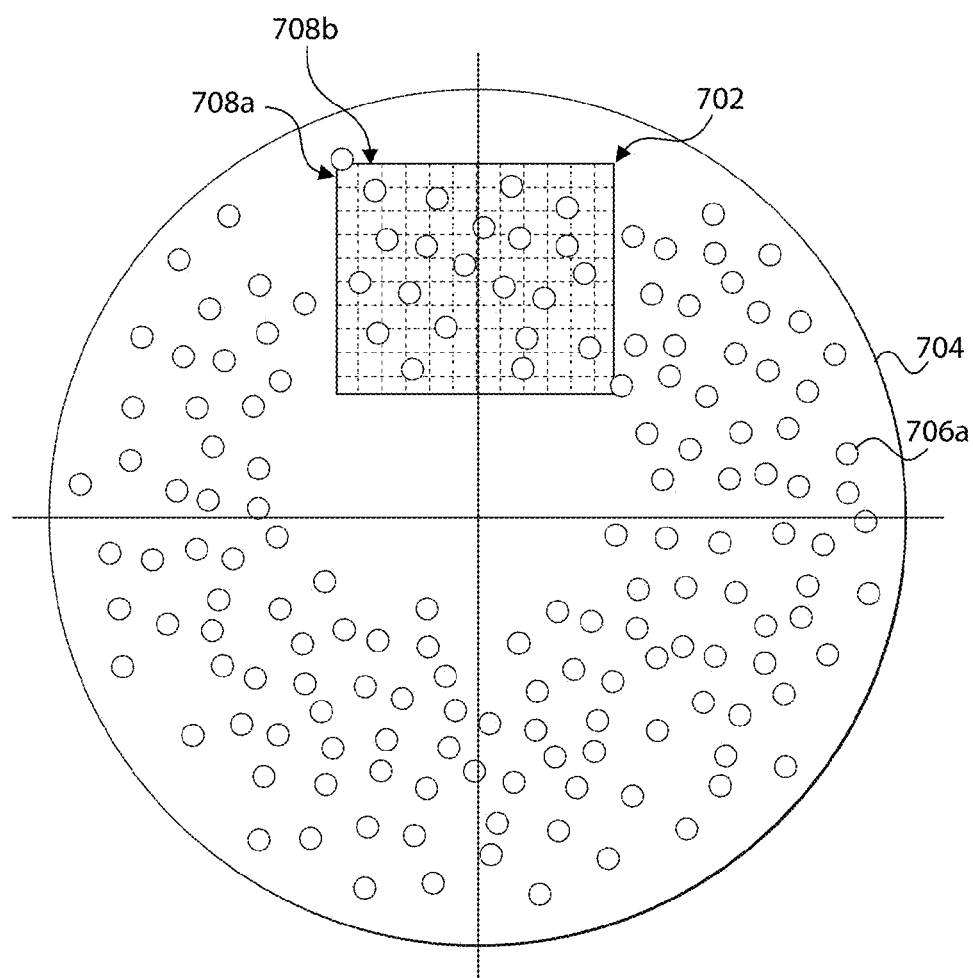


Fig. 7

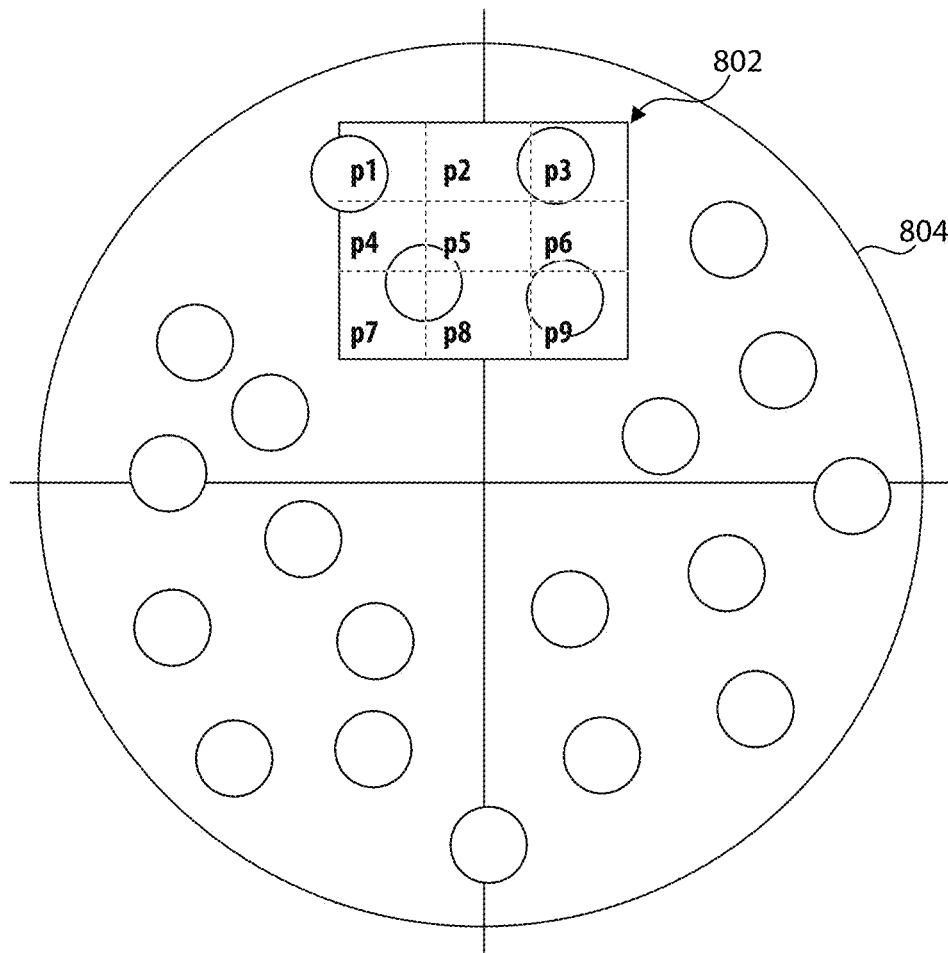


Fig. 8

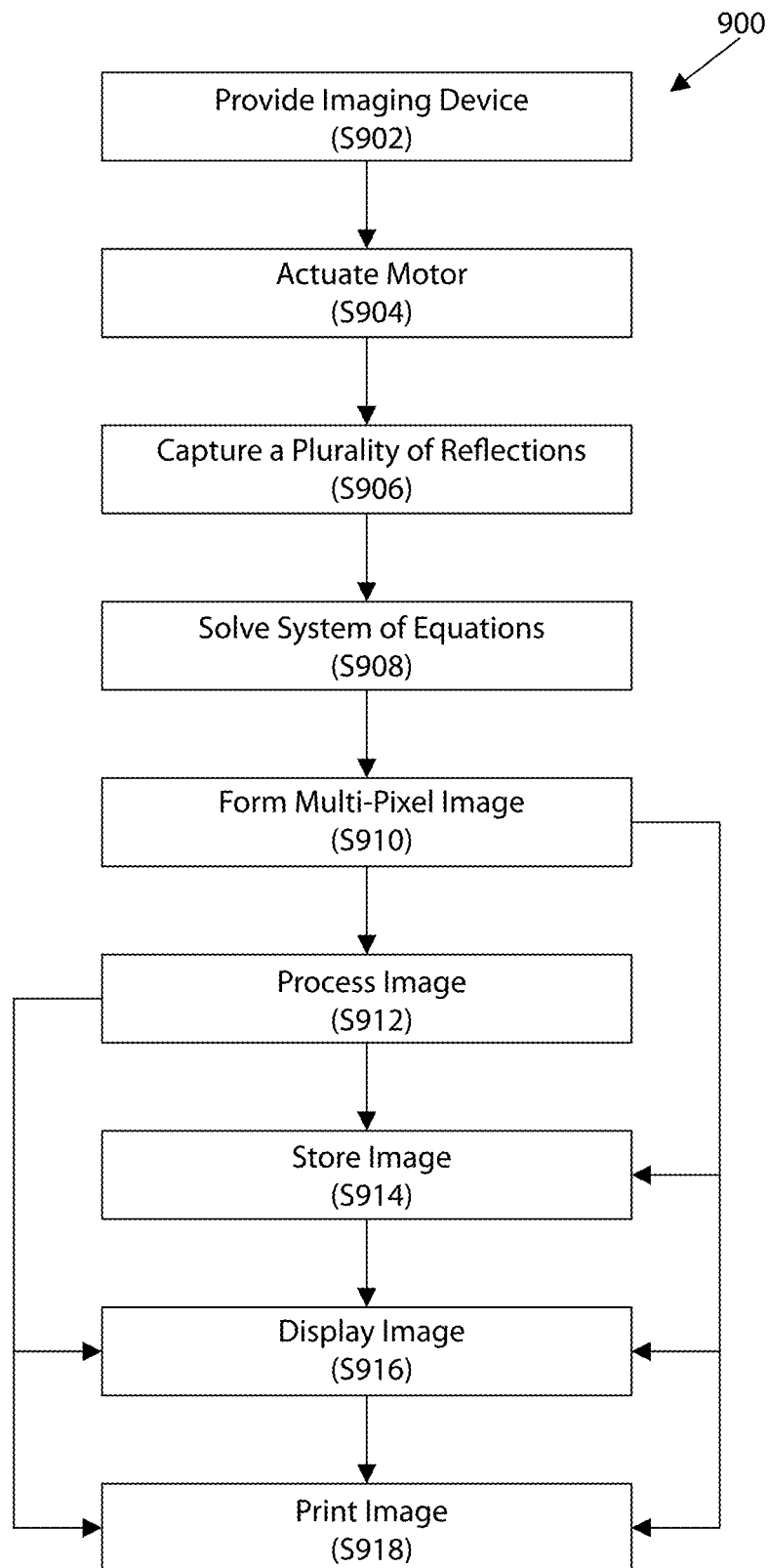


Fig. 9

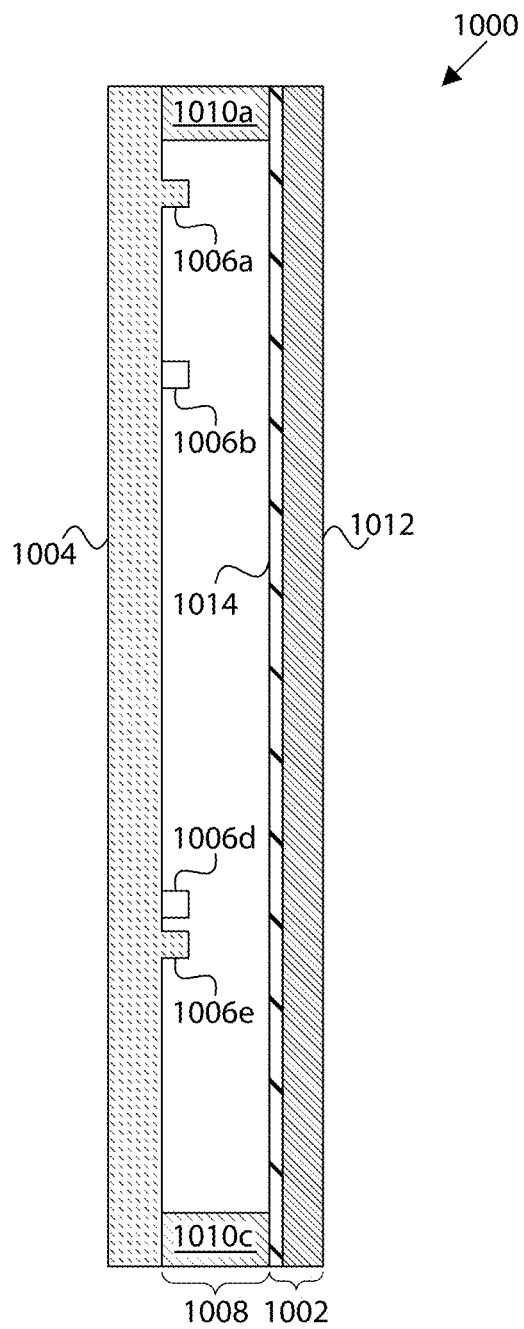


Fig. 10

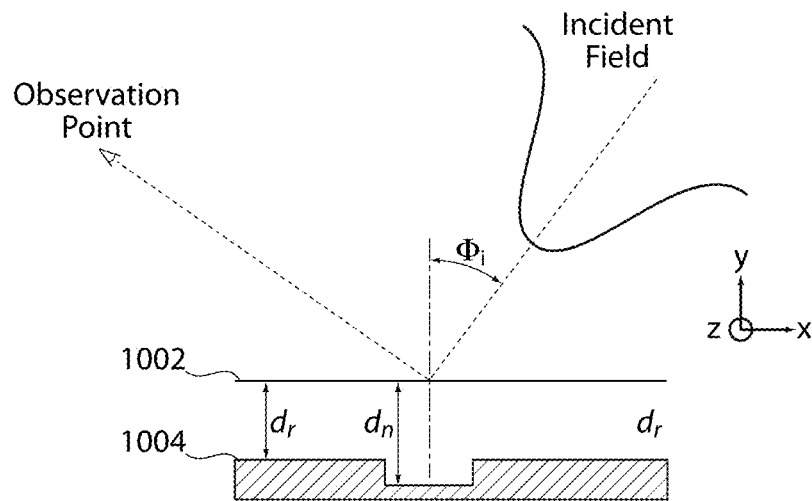


Fig. 11A

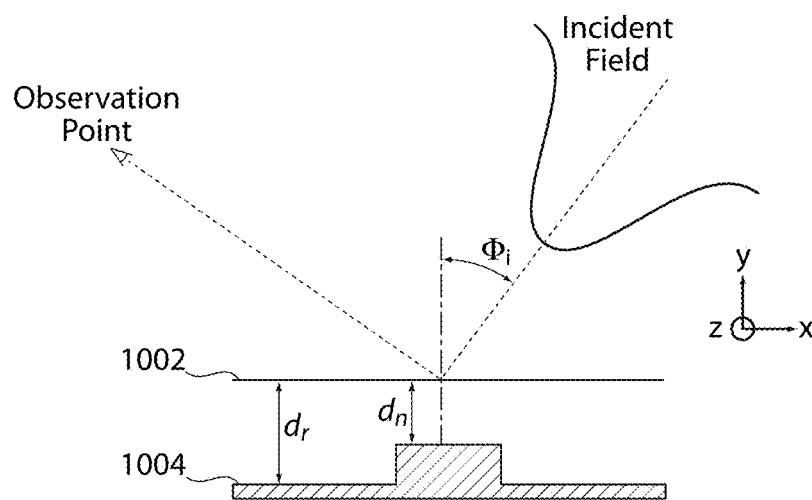


Fig. 11B

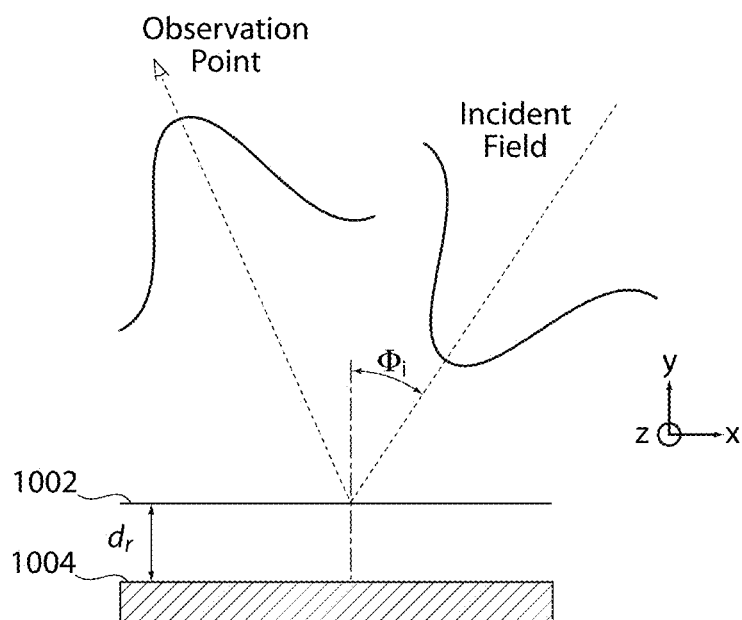


Fig. 11C

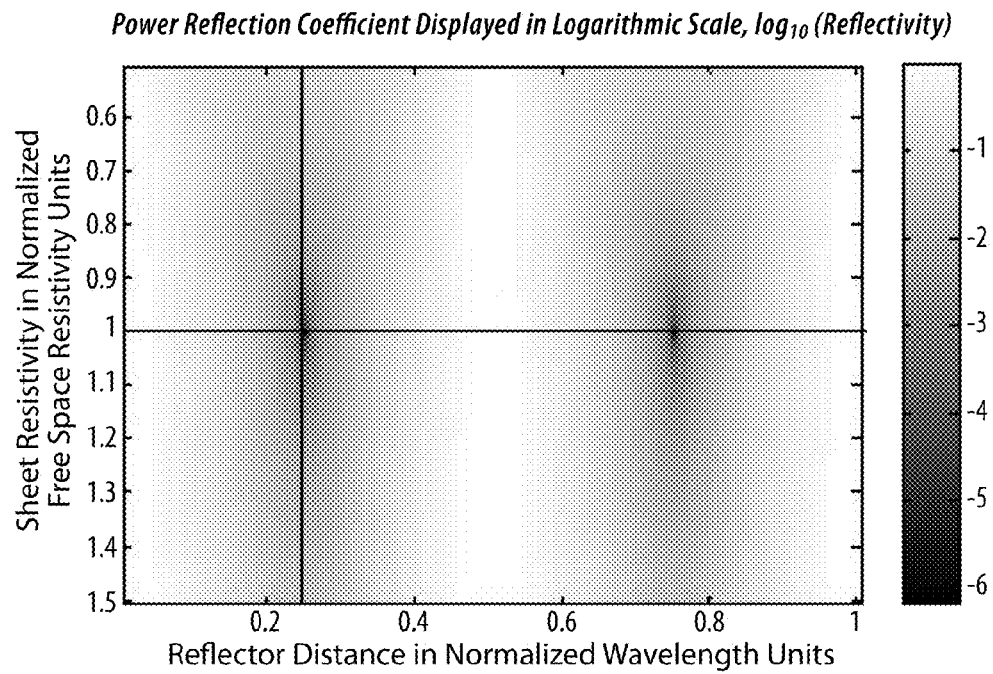


Fig. 12A

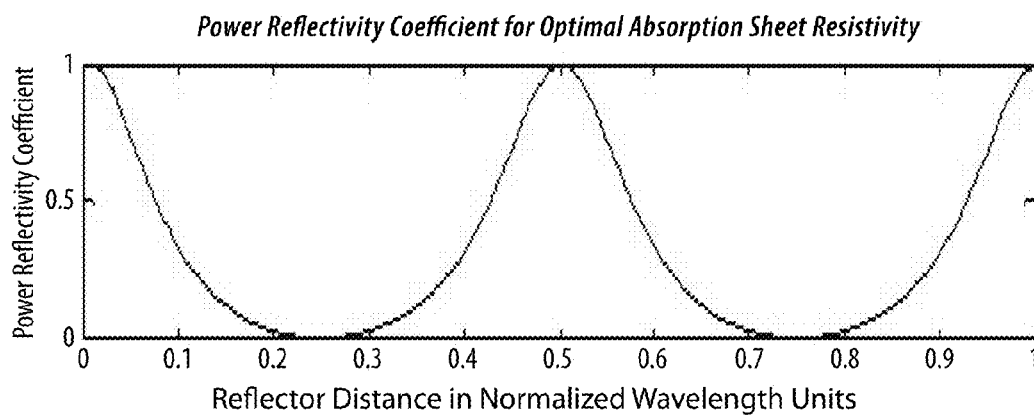


Fig. 12B

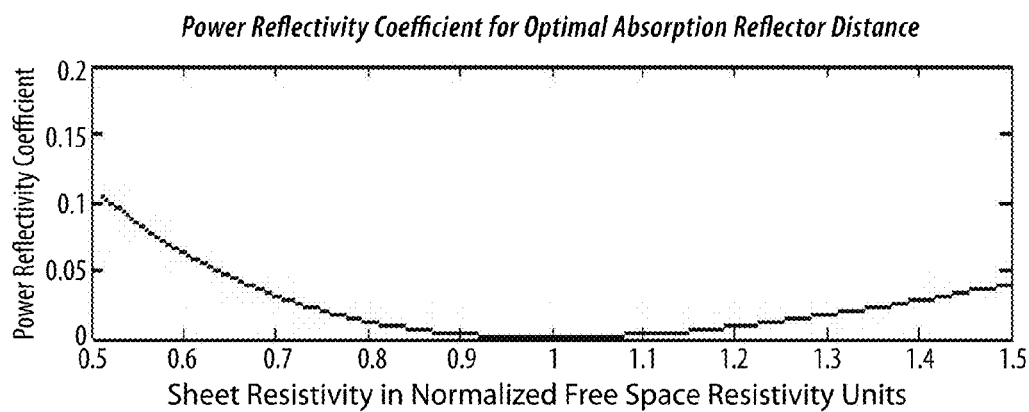


Fig. 12C

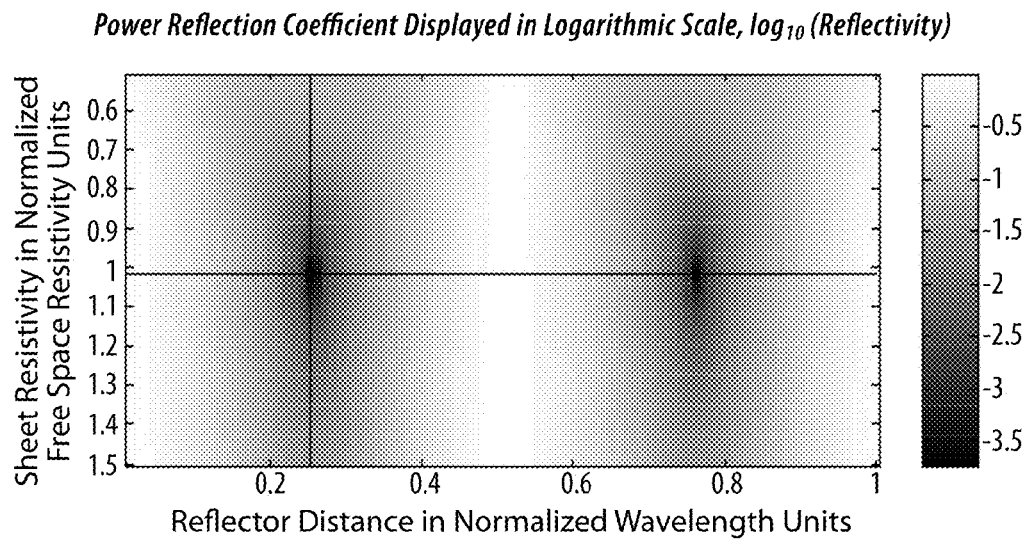


Fig. 12D

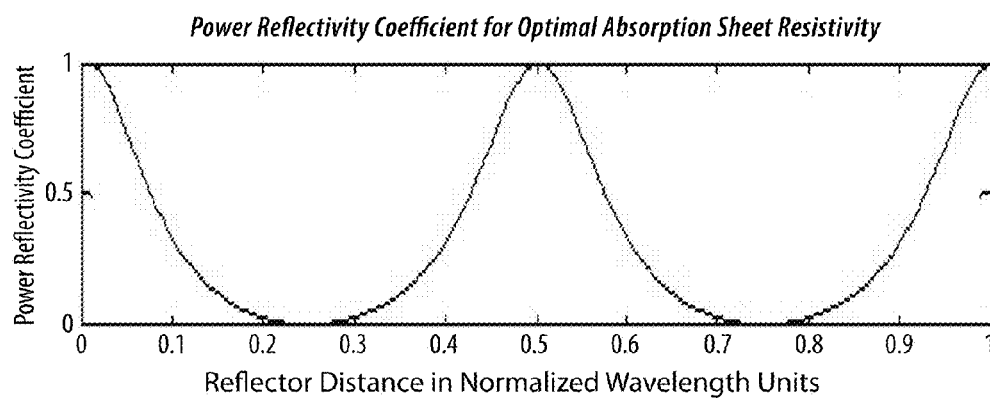


Fig. 12E

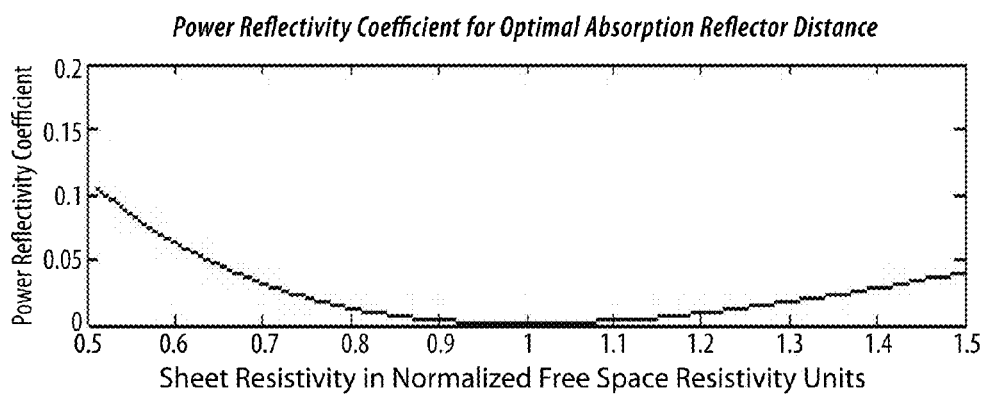


Fig. 12F

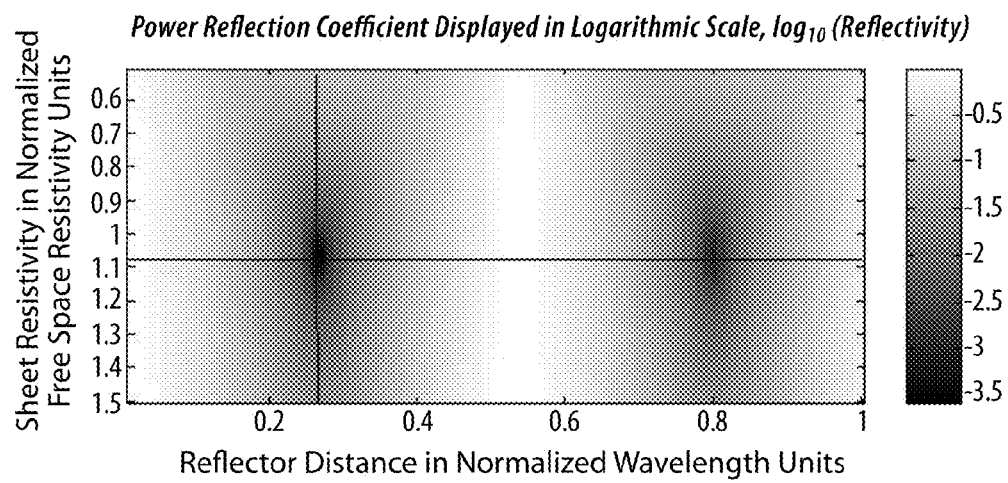


Fig. 12G

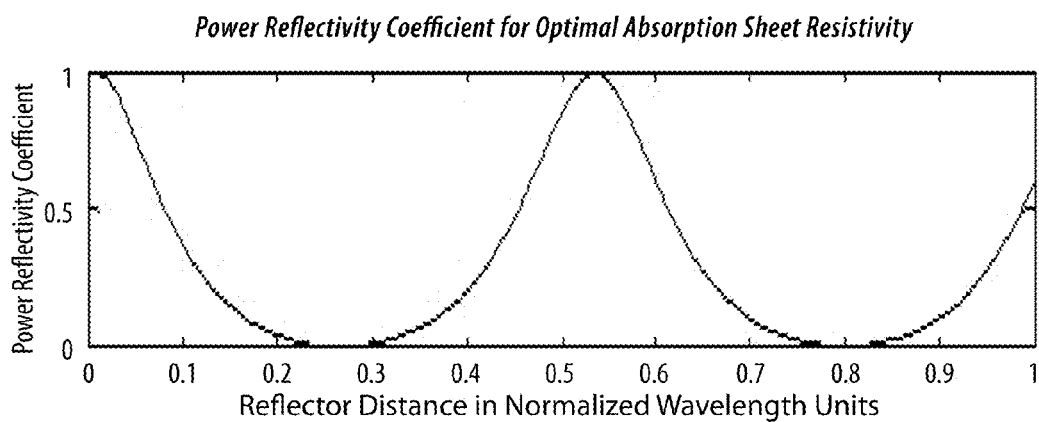


Fig. 12H

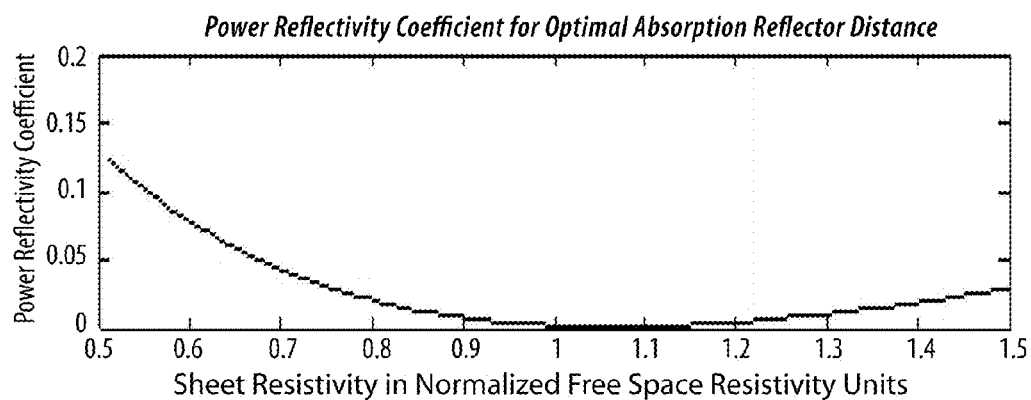


Fig. 12I

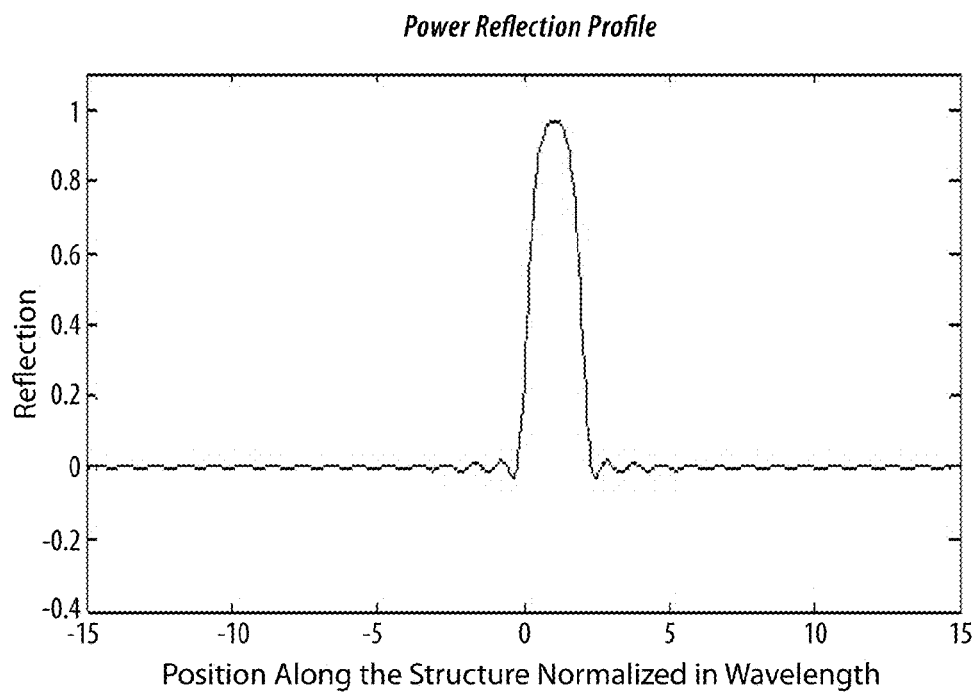


Fig. 13A

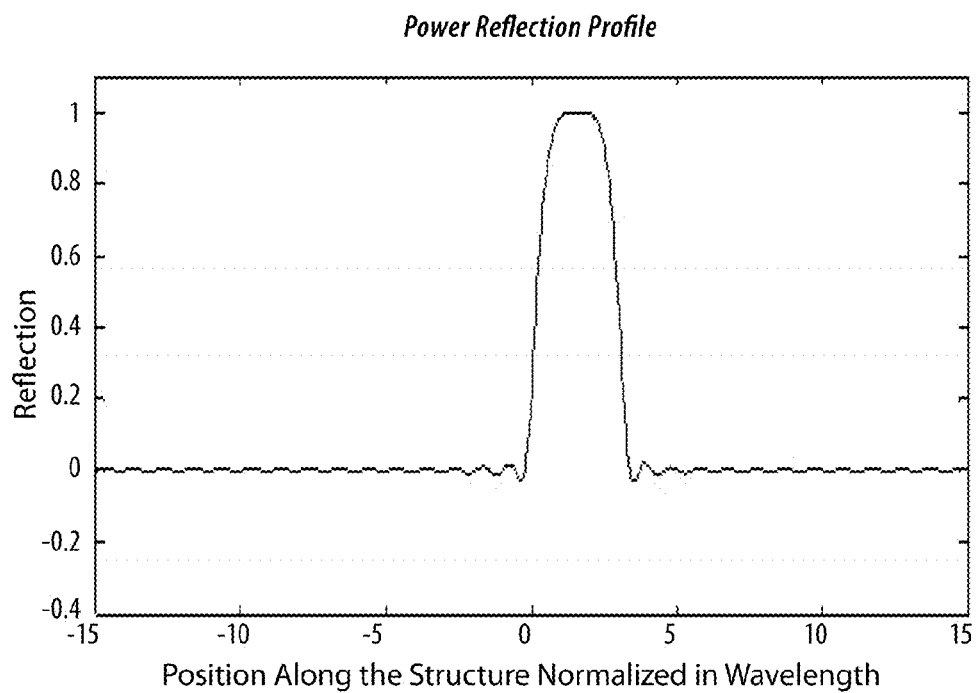
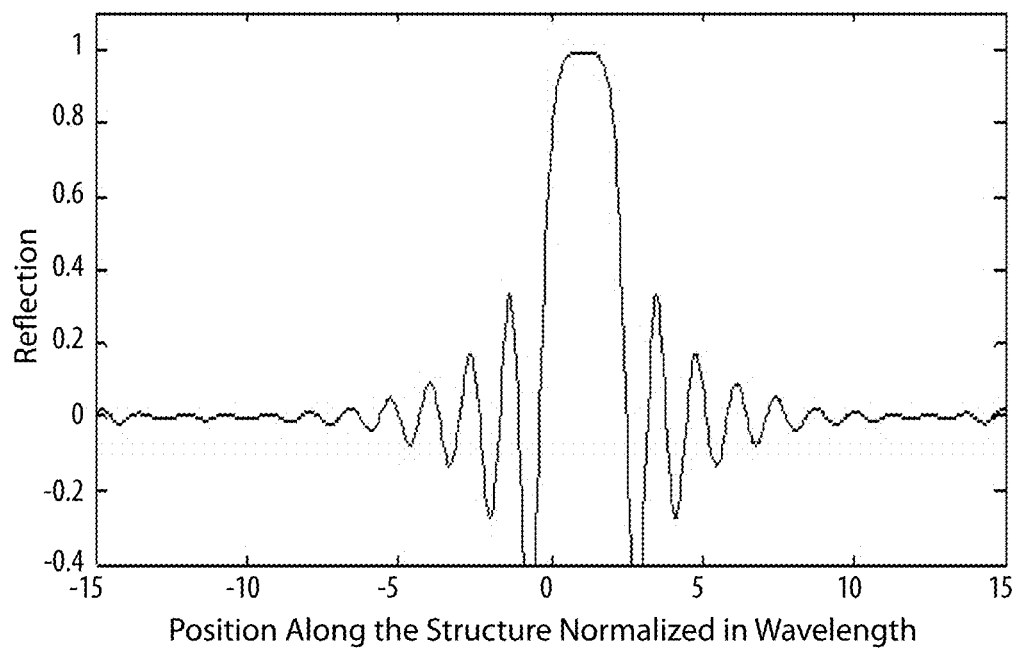
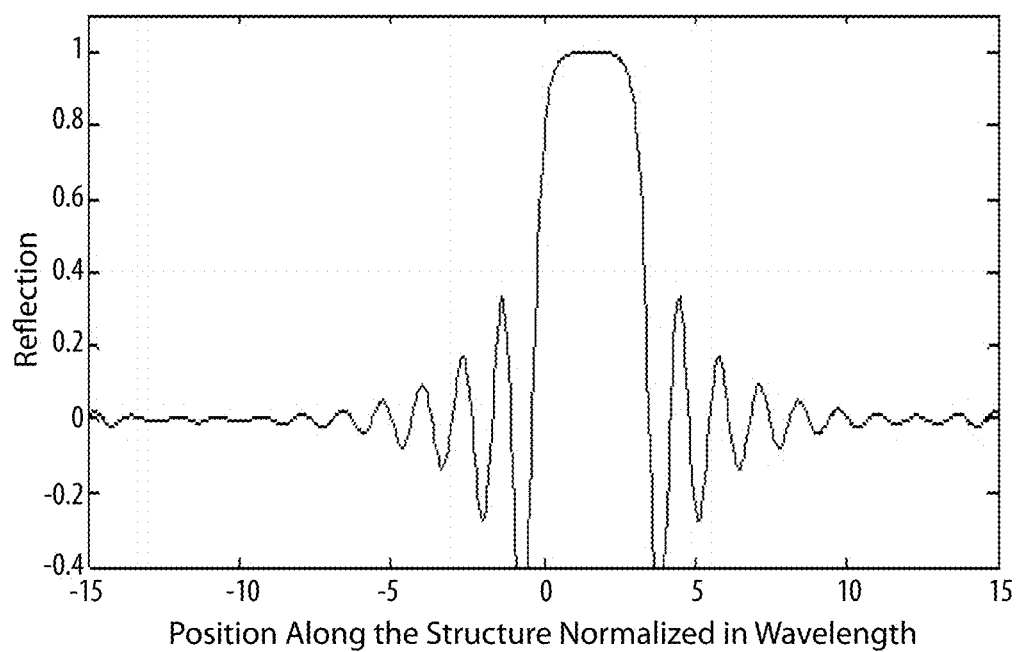


Fig. 13B

Power Reflection Profile**Fig. 14A***Power Reflection Profile***Fig. 14B**

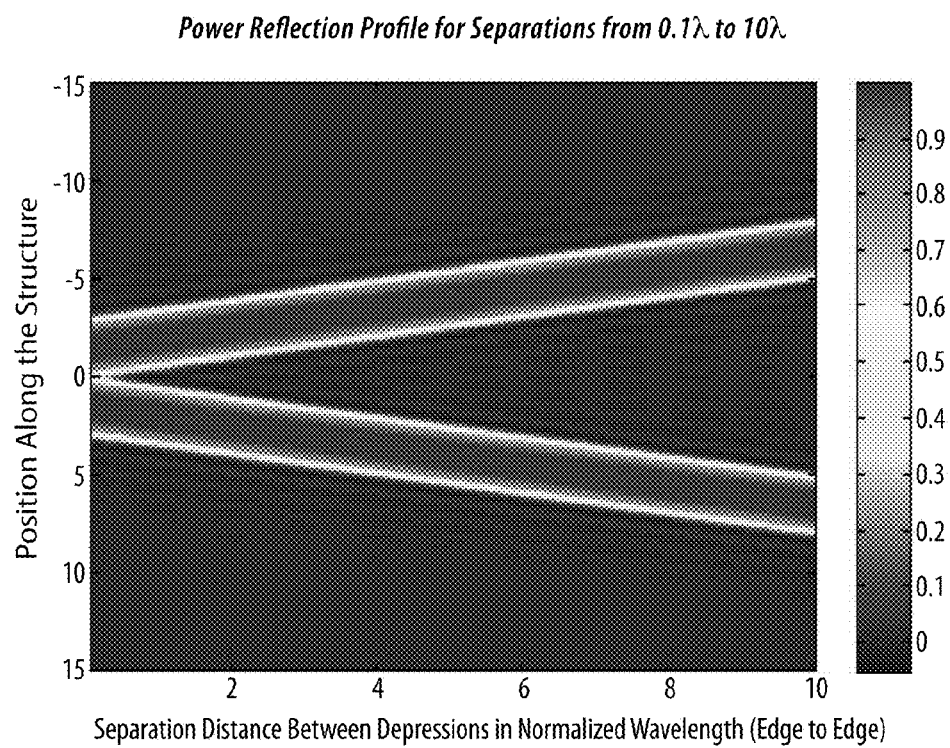


Fig. 15

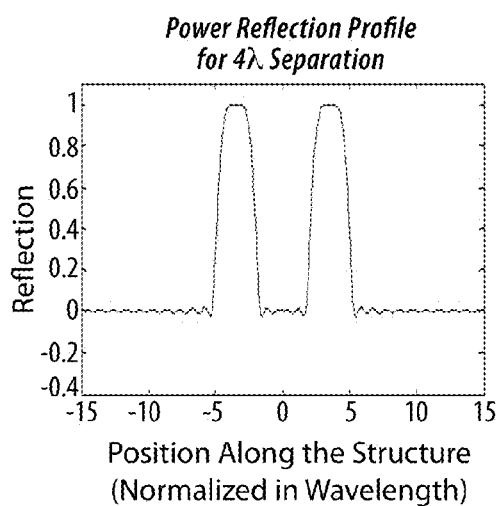


Fig. 16A

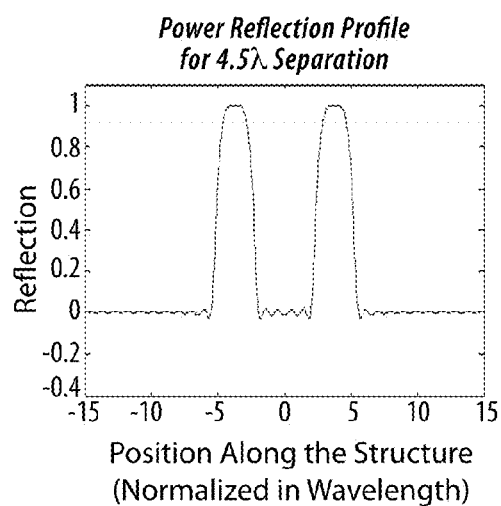


Fig. 16B

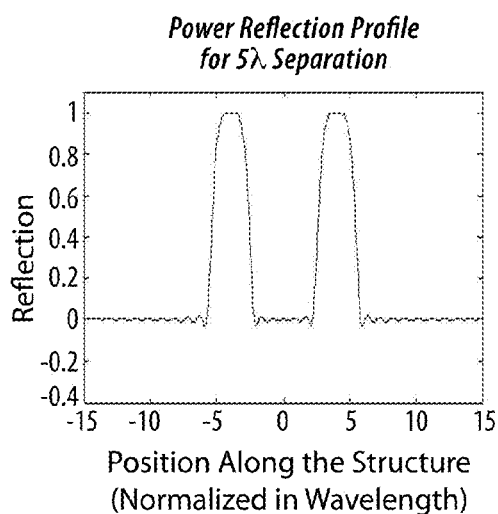


Fig. 16C

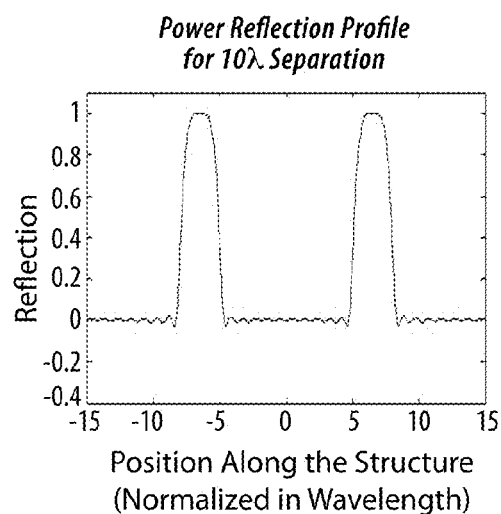


Fig. 16D

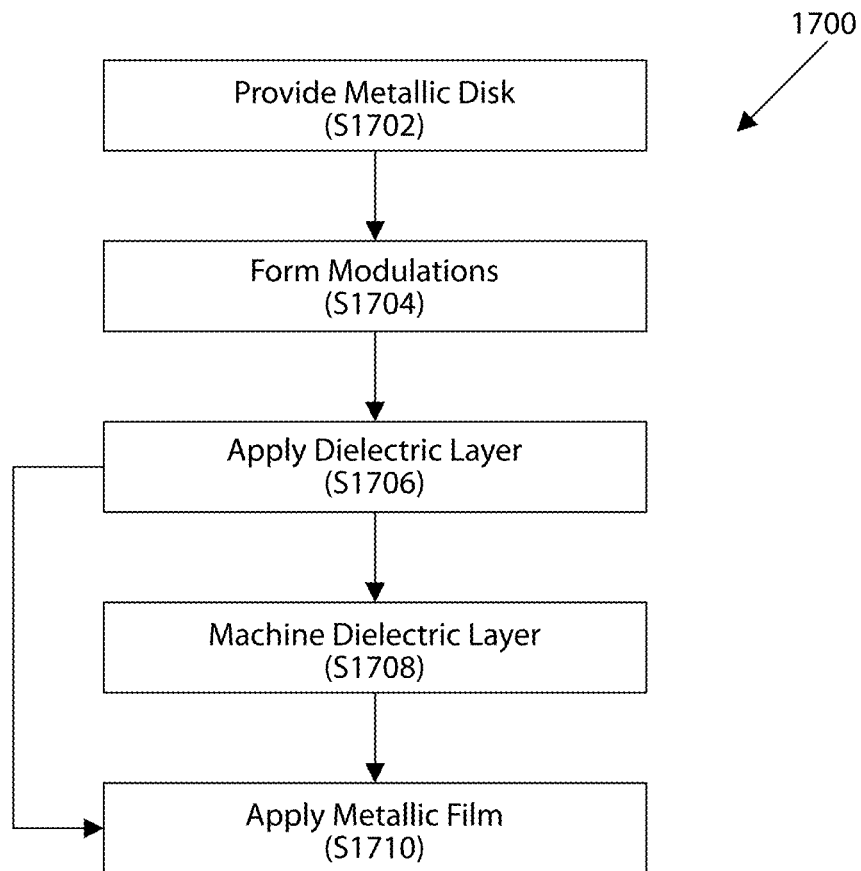


Fig. 17

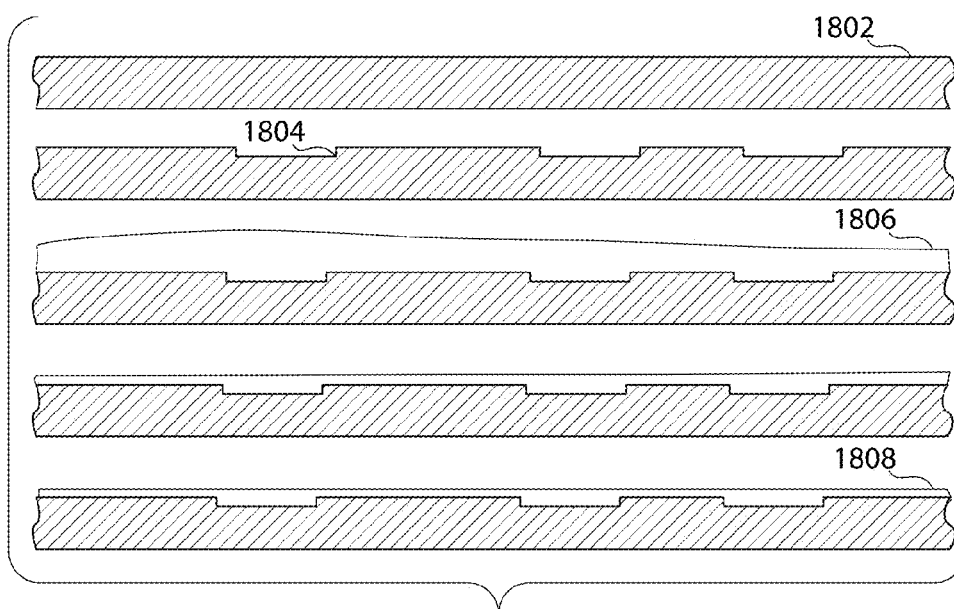


Fig. 18

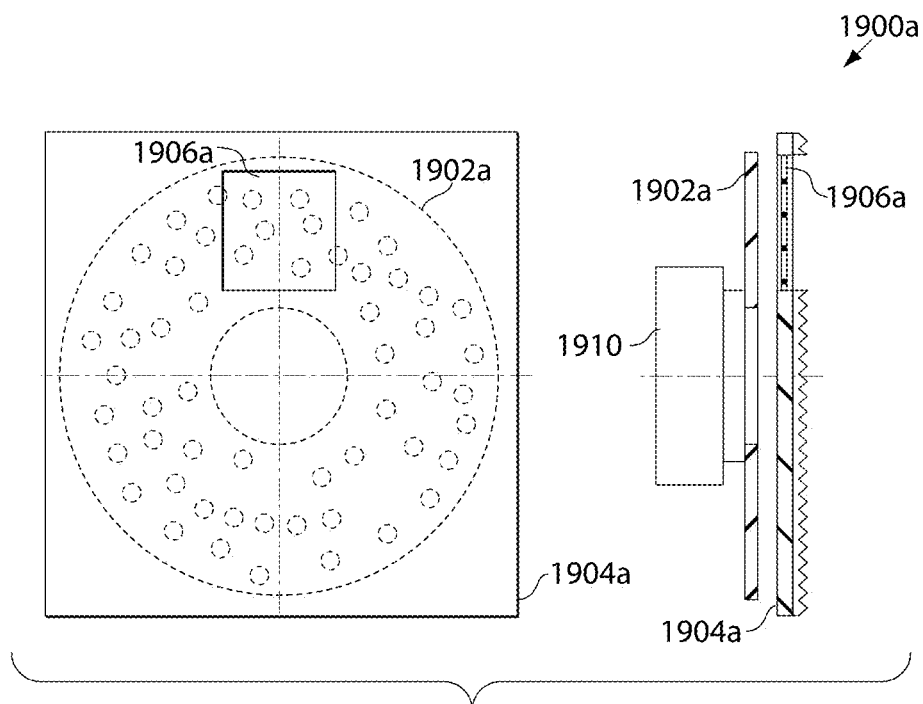


Fig. 19A

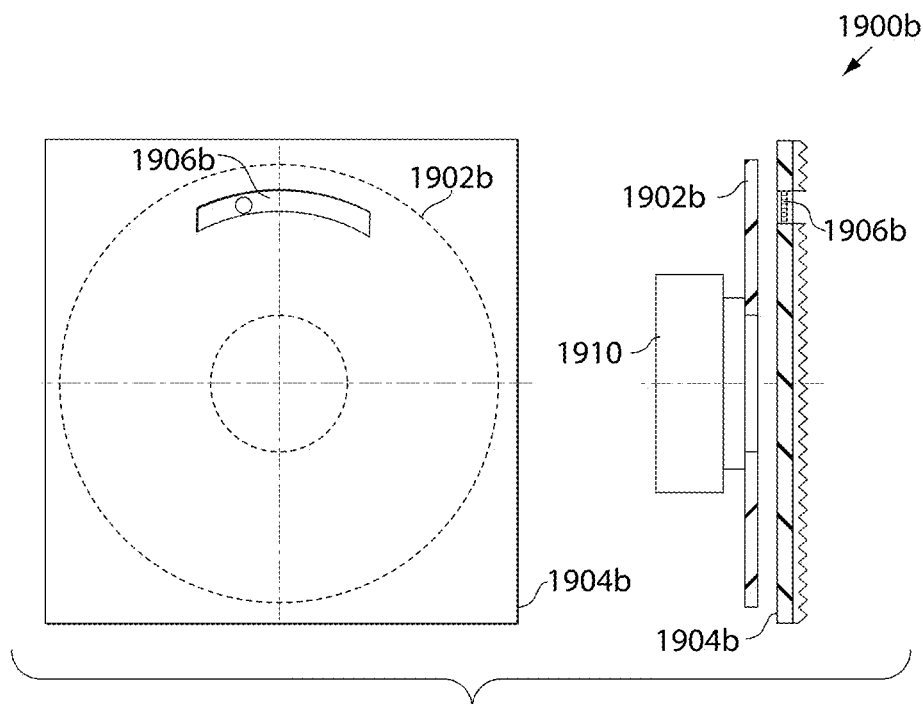


Fig. 19B

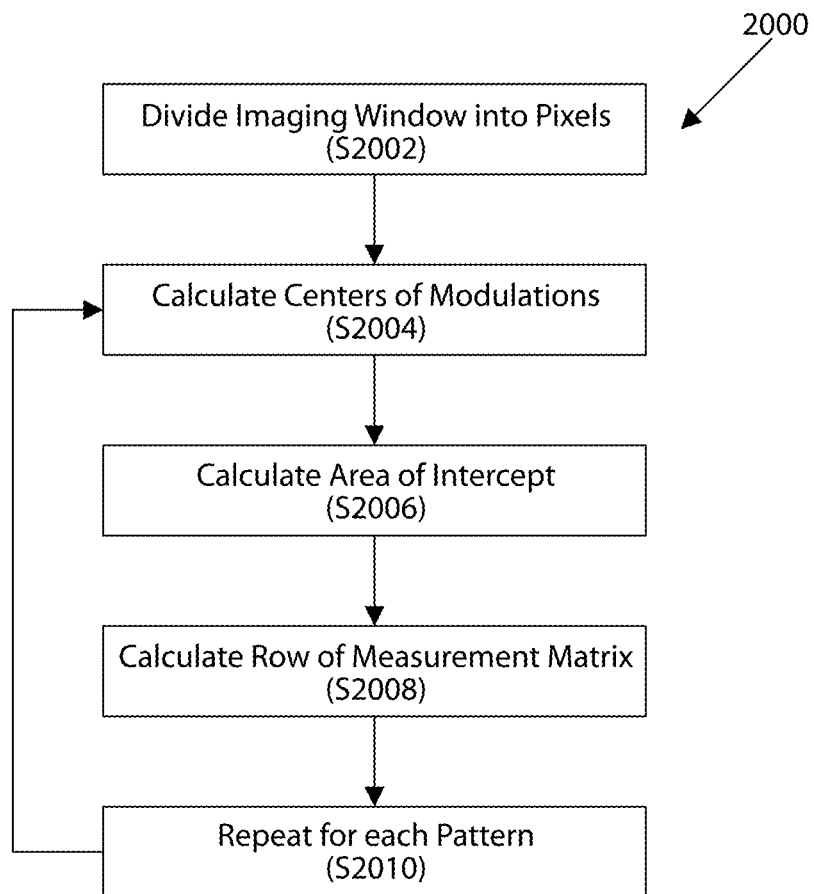


Fig. 20

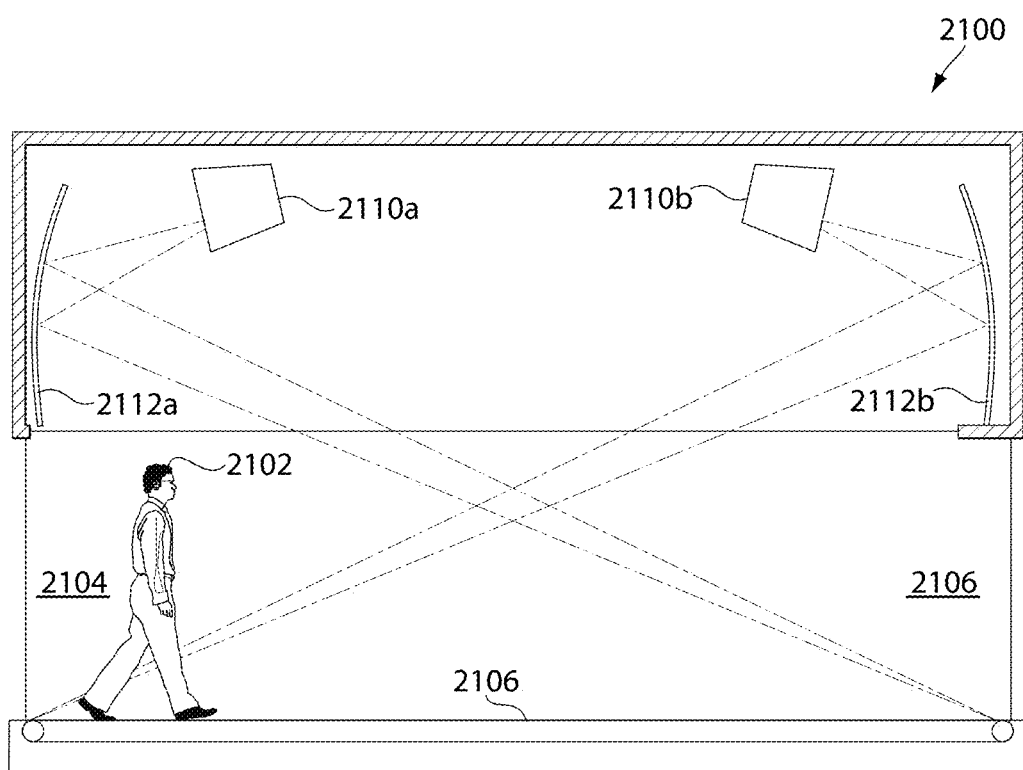


Fig. 21

1

SPATIALLY-SELECTIVE REFLECTOR STRUCTURES, REFLECTOR DISKS, AND SYSTEMS AND METHODS FOR USE THEREOF

CROSS-REFERENCES TO RELATED APPLICATION

This application is a continuation under 35 U.S.C. §120 of U.S. patent application Ser. No. 12/713,049, filed Feb. 25, 2010, which claims priority under 35 U.S.C. §119(e) to U.S. Provisional Patent Application Ser. No. 61/155,316, filed Feb. 25, 2009, and U.S. Provisional Patent Application Ser. No. 61/301,433, filed Feb. 4, 2010. The contents of these patent applications are hereby incorporated by reference in their entirety.

BACKGROUND

Terrorist attacks over the last decade have heightened security requirements at a host of locations and activities such as airports, sporting events, political gatherings, and the like. Security stations at these locations must process large numbers of individuals in an efficient manner while providing effective screening for weapons and contraband.

Screening for concealed weapons is a particularly challenging task. Many individuals have a variety of metallic items in or on their person (e.g. prostheses, jewelry, belt buckles, coins), thereby impairing the effectiveness of conventional metal detectors. Moreover, weapons can be fabricated from non-metallic materials that cannot be detected with conventional metal detectors. Backscatter X-ray devices exist for detecting such concealed devices, but require that an individual stand close to a flat panel and raise health concerns due to ionizing radiation exposure.

Accordingly, it would be desirable to provide a device that provides improved-resolution imaging of concealed objects without the need for ionizing radiation.

SUMMARY OF THE INVENTION

The invention provides a spatially-selective reflective structure for the detection of submillimeter electromagnetic waves and systems and methods incorporating spatially-selective reflective structures.

One aspect of the invention provides a spatially-selective reflective structure including a partially-conducting slab and a modulating reflector disk adjacent to the partially-conducting slab. The modulating reflector disk includes one or more modulations.

This aspect of the invention can have several embodiments. The one or more modulations can be a single modulation. The one or more modulations can be a plurality of modulations. The plurality of modulations can be arranged in a spiral pattern. The plurality of modulations can be arranged randomly.

The plurality of modulations can be arranged such that a matrix having a plurality of rows, each with elements corresponding to a fraction of each pixel in a viewing window projected onto the disk that is backed by a modulation at a distinct rotational position of the disk, has linearly independent rows.

The plurality of modulations can be separated by a multiple of a wavelength of interest. The multiple can be an odd multiple. The multiple can be greater than five.

The modulations can have well-defined edges. The partially-conducting slab can be a semiconductor. The partially-

2

conducting slab can be a dielectric doped with conductive particles. The partially-conducting slab can include a non-conductive plate and a thin metal film applied to the non-conductive plate.

The modulating reflector disk can include a highly-conductive metal. The partially-conducting slab and the modulating reflector disk can be coupled with one or more mechanical fasteners. The modulating reflector disk can rotate independently of the partially-conducting slab.

The partially-conducting slab and the modulating reflector disk can be separated by a gap. The gap can be adjustable. The modulations can be depressions or bumps.

The modulations can have a cross-sectional dimension greater or equal to about one wavelength of interest. The one or more modulations can have a cross-sectional dimension greater or equal to three wavelengths of interest. The one or more modulations can have a cross-sectional dimension less than the wavelength of interest multiplied by an F-number for an optics system directing radiation at the spatially-selective reflective structure.

The distance between the modulations of the modulating reflector disk and the partially-conducting slab can be defined by the formula

$$d_n = n \frac{\lambda}{2\sqrt{\epsilon_r \cos(\phi_i)}},$$

$$n = 1, 2, \dots,$$

wherein ϵ_r is the relative permittivity of the media between the partially-conducting slab and the modulations, λ is the wavelength of interest, and ϕ_i is the angle of radiation incidence given with respect to a normal of the spatially-selective reflective structure.

The distance between a non-modulated surface of the modulating reflector disk and the partially-conducting slab can be defined by the formula

$$d_r = \frac{(2n-1)\lambda}{4\sqrt{\epsilon_r \cos(\phi_i)}},$$

$$n = 1, 2, \dots$$

wherein ϵ_r is the relative permittivity of the media between the partially-conducting slab and the modulations, λ is the wavelength of interest, and ϕ_i is the angle of radiation incidence given with respect to a normal of the spatially-selective reflective structure.

Another aspect of the invention provides a submillimeter imaging device including submillimeter wave optics, a spatially-selective reflective structure located in the focal plane of the submillimeter wave optics, a submillimeter wave receiver positioned to capture waves reflected from the spatially-selective reflective structure, and a motor configured to rotate the spatially-selective reflective structure. The spatially-selective reflective structure includes a partially-conducting slab and a modulating reflector disk adjacent to the partially-conducting slab. The modulating reflector plate includes one or more modulations.

This aspect of the invention can have several embodiments. The device can further include a submillimeter wave source. The spatially-selective reflective structure can be positioned to selectively reflect submillimeter waves from an image formed on the spatially-selective reflective structure by the

submillimeter wave optics to the submillimeter wave receiver. The submillimeter wave optics can include a focusing mirror. The motor can rotate the spatially-selective reflective structure at about 1,800 revolutions per minute. The receiver can capture images at a rate of about 30 frames per second.

The plurality of modulations can be arranged in a spiral pattern. The plurality of modulations can be arranged in randomly. The plurality of modulations can be arranged such that a matrix having a plurality rows, each with elements corresponding to a fraction of each pixel in a viewing window projected onto the disk that is backed by a modulation at a distinct rotational position of the disk, has linearly independent rows. The submillimeter imaging device can include a shield defining a viewing window on the spatially-selective reflective structure.

Another aspect of the invention provides a method of submillimeter imaging. The method includes providing submillimeter wave optics, a spatially-selective reflective structure located in the focal plane of the submillimeter wave optics, a submillimeter wave receiver positioned to capture waves reflected from the spatially-selective reflective structure, and a motor configured to rotate the spatially-selective reflective structure; actuating the motor to rotate the spatially-selective reflective structure; capturing a plurality of reflections from the plurality of modulations as the spatially-selective reflective structure rotates; storing each of the plurality of reflections as a pixel; and forming an image from the plurality of the pixels. The spatially-selective reflective structure includes a partially-conducting slab and a modulating reflector disk adjacent to the partially-conducting slab. The modulating reflector plate includes a plurality of modulations.

This aspect of the invention can have several embodiments. The method can include storing the image, displaying the image, and/or performing an image recognition method on the image. The storing and forming steps can be performed on a computer.

Another aspect of the invention provides a method of submillimeter imaging. The method includes: providing submillimeter wave optics, a spatially-selective reflective structure located in the focal plane of the submillimeter wave optics, a submillimeter wave receiver positioned to capture waves reflected from the spatially-selective reflective structure, and a motor configured to rotate the spatially-selective reflective structure; actuating the motor to rotate the spatially-selective reflective structure; capturing a plurality of reflections from the plurality of modulations as the spatially-selective reflective structure rotates; solving a system of equations wherein a magnitude of one of the plurality of reflections is equal to a sum of a product of the reflection in each of a plurality of pixels and the fraction of pixel area backed by the plurality of modulations; and forming an image from the plurality of the pixels. The spatially-selective reflective structure includes a partially-conducting slab and a modulating reflector disk adjacent to the partially-conducting slab. The modulating reflector plate includes a plurality of modulations.

This aspect of the invention can have several embodiments. The number of equations in the system of equations can be equal to the number reflections captured. The plurality of modulations can be arranged such that a matrix having a plurality rows, each with elements corresponding to a fraction of each pixel in a viewing window projected onto the disk that is backed by a modulation at a distinct rotational position of the disk, has linearly independent rows. The solving and forming steps can be performed on a computer.

Another aspect of the invention provides a reflector disk including a metal disk having one or more modulations, a dielectric coupled to the metal disk, and a metal film coupled to the dielectric.

Another aspect of the invention provides a method of fabricating a reflector disk. The method includes applying a dielectric to a metal disk having one or more modulations and applying a metal film to the dielectric.

This aspect of the invention can have a variety of embodiments. The method can include forming the one or more modulations. The method can include machining the dielectric to produce uniform surface prior to applying the metal film.

Another aspect of the invention provides a profiling scanner including a proximal end, a distal end, a first submillimeter imaging device, and a second submillimeter imaging device. The first submillimeter imaging device includes: a first spatially-selective reflective structure, a first submillimeter wave receiver positioned to capture waves reflected from the first spatially-selective reflective structure, and a first motor configured to rotate the first spatially-selective reflective structure. The first spatially-selective reflective structure includes a first partially-conducting slab and a first modulating reflector disk adjacent to the first partially-conducting slab. The first modulating reflector plate includes one or more modulations. The second submillimeter imaging device includes: a second spatially-selective reflective structure, a second submillimeter wave receiver positioned to capture waves reflected from the second spatially-selective reflective structure, and a second motor configured to rotate the second spatially-selective reflective structure. The second spatially-selective reflective structure includes a second partially-conducting slab and a second modulating reflector disk adjacent to the second partially-conducting slab. The second modulating reflector plate includes one or more modulations.

This aspect of the invention can have a variety of the embodiments. In one embodiment, the profiling scanner includes a moving walkway configured to carry an individual from the proximal end to the distal end.

FIGURES

For a fuller understanding of the nature and desired objects of the present invention, reference is made to the following detailed description taken in conjunction with the accompanying drawing figures wherein:

FIGS. 1A and 1B depict a side view and a cross-sectional view, respectively, of a spatially-selective reflective structure according to one embodiment of the invention.

FIG. 1C depicts a reflecting disk with a plurality of modulations arranged in a single-turn spiral according to one embodiment of the invention.

FIGS. 2A-2F depict several modulation profiles according to some embodiments of the invention.

FIG. 3A depicts an imaging system incorporating a spatially-selective reflective structure according to one embodiment of the invention.

FIG. 3B depicts an imaging system incorporating a spatially-selective reflective structure and radar absorbing material according to one embodiment of the invention.

FIG. 3C depicts an imaging system incorporating a spatially-selective reflective structure and a beam splitter according to one embodiment of the invention.

FIG. 3D depicts an imaging system incorporating a spatially-selective reflective structure and secondary optics according to one embodiment of the invention.

5

FIGS. 4A-4C depict the acquisition of an image according to one embodiment of the invention.

FIG. 5 depicts an imaging method according to one embodiment of the invention.

FIG. 6A depicts a three layer model for reflectivity of the spatially-selective reflective structure according to one embodiment of the invention.

FIG. 6B depicts reflection coefficient Γ as a function of gap distance, partially-conductive slab thickness, and partially-conductive slab conductivity.

FIG. 7 depicts an embodiment of a modulating reflector disk including a plurality of randomly-positioned modulations.

FIG. 8 depicts an exaggerated modulating reflector disk and a nine-pixel viewing window.

FIG. 9 depicts a method of creating a multi-pixel image according to one embodiment of the invention.

FIG. 10 depicts a partially-conducting slab including a non-conductive material coated with a thin metallic film according to one embodiment of the invention.

FIGS. 11A-11C depict schematics for reflective structures having depressions, bumps, and no modulations, respectively, according to various embodiments of the invention.

FIGS. 12A-12I depict the power reflectivity coefficient as function of reflector distance and/or sheet resistance for various radiation incidence angles according to various embodiments of the invention.

FIGS. 13A and 13B depict the power reflection profile of a spatially-selective reflective structure having a depression of linear dimensions 2λ and 3λ respectively, for a reflective structure wherein the depression distance and reflector distance from the resistive sheet are

$$\frac{\lambda}{2} \text{ and } \frac{\lambda}{4},$$

respectively, the sheet resistivity is $377\Omega/\square$, and the radiation is normally incident to the structure according various embodiments of the invention.

FIGS. 14A and 14B depict the power reflection profile of a spatially-selective reflective structure having a bump distance and reflector distance of

$$\frac{\lambda}{2} \text{ and } \frac{3\lambda}{4},$$

respectively, a sheet resistivity of $377\Omega/\square$, and radiation normally incident to the structure according various embodiments of the invention

FIG. 15 depicts the power reflection coefficient for a structure that is modulated by two depressions separated by a gap that varies from 0.1λ to 10λ according to various embodiments of the invention.

FIGS. 16A, 16B, 16C, and 16D depict slices of FIG. 15 and provide reflectivity profiles for separations of 4λ , 4.5λ , 5λ , and 10λ , respectively, according to various embodiments of the invention.

FIG. 17 depicts a method of fabricating a reflector disk according to one embodiment of the invention.

FIG. 18 depicts the fabrication of a reflector disk according to one embodiment of the invention.

FIGS. 19A and 19B depict spatially-selective reflector device and motor assemblies according to various embodiments of the invention.

6

FIG. 20 depicts a method for calculating a measurement matrix according to an embodiment of the invention.

FIG. 21 depicts a profiling scanner incorporating the imaging devices described herein according to an embodiment of the invention.

DESCRIPTION OF THE INVENTION

Spatially-selective reflective structures are described along with systems and methods utilizing spatially-selective reflective structures. The spatially-selective reflective structures can be used to image targets using electromagnetic energy of a various wavelengths referred to herein as the "wavelength(s) of interest."

Spatially-Selective Reflective Structures

FIGS. 1A and 1B depict a side view and a cross-sectional view, respectively, of a spatially-selective reflective structure **100** according to one embodiment of the invention. Spatially-selective reflective structure **100** includes a partially-conducting slab **102** and a modulating reflector disk **104**. The modulating reflector disk **104** includes a plurality of modulations **106a-h**.

Modulations **106a-h** are preferably uniform in size and shape. The modulations can be designed to maximally perturb the absorption properties of the partially-conducting slab **102** and reflector disk **104**. Preferably, the modulations have well-defined edges, as depicted in FIG. 1A, which promote energy reflection. While particular sizes and shapes are not required, exemplary modulations can, in some embodiments, have a cross-sectional dimension greater or equal to about one wavelength of interest and extend above or below the surface of modulating reflector disk **104**.

The height or depth of the modulations **106** is generally about less than a wavelength of interest or a multiple of a half of one wavelength of interest plus about less than a half of one wavelength of interest. For example, modulation height H can be defined by the following formula:

$$H \approx n_m \frac{\lambda}{2} + d_m \frac{\lambda}{2} \quad (1)$$

wherein n_m is a non-negative integer, λ is the wavelength of interest, and $0 \leq d_m \leq 1$. Parameter d_m will vary depending on the properties of the partially-conducting slab **102** (e.g. the thickness of the slab **102**, the electrical conductivity of the slab **102**, and the electrical permittivity of the slab **102**). For example, if a slab **102** is provided with a uniform electrical conductivity of 0.066 S/cm , thickness of $820 \mu\text{m}$, and relative electrical permittivity of 11.9 F/m , and the frequency of interest is 640 GHz ($\lambda=468.75 \mu\text{m}$), the desired bump height H_b (i.e., the distance from surface of the partially-conducting slab z_2 to the surface of bump z_{3a} as depicted in FIG. 6A) for maximal reflection of radiation can be defined as follows:

$$H_b \approx n_m \frac{\lambda}{2} + \frac{47}{2} \mu\text{m} \approx n_m \frac{\lambda}{2} + 0.1 \frac{\lambda}{2}. \quad (2)$$

The desired depression depth H_d (i.e., the distance from the surface of the partially-conducting slab to the depression

surface) for maximal reflection of radiation for the such a slab can be defined as follows:

$$H_d \approx n_m \frac{\lambda}{2} + \frac{347}{2} \mu\text{m} \approx n_m \frac{\lambda}{2} + 0.4 \frac{\lambda}{2}. \quad (3)$$

The partially-conducting slab **102** can be composed of a semiconductor materials including but not limited to: diamond, silicon, germanium, silicon carbide, silicon germanide, aluminum antimonide, aluminum arsenide, aluminum nitride, aluminum phosphide, boron nitride, boron phosphide, boron arsenide, gallium antimonide, gallium arsenide, gallium nitride, gallium phosphide, indium antimonide, indium arsenide, indium nitride, indium phosphide, aluminum gallium arsenide, indium gallium arsenide, indium gallium phosphide, aluminum indium arsenide, aluminum indium antimonide, gallium arsenide nitride, gallium arsenide phosphide, aluminum gallium nitride, aluminum gallium phosphide, indium gallium nitride, indium arsenide antimonide, indium gallium antimonide, aluminum gallium indium phosphide, aluminum gallium arsenide phosphide, indium gallium arsenide phosphide, aluminum indium arsenide phosphide, aluminum gallium arsenide nitride, indium gallium arsenide nitride, indium aluminum arsenide nitride, gallium arsenide antimonide nitride, gallium indium nitride arsenide antimonide, gallium indium arsenide antimonide phosphide, cadmium selenide, cadmium sulfide, cadmium telluride, zinc oxide, zinc selenide, zinc sulfide, zinc telluride, cadmium zinc telluride, mercury cadmium telluride, mercury zinc telluride, mercury zinc selenide, cuprous chloride, lead selenide, lead sulfide, lead telluride, tin sulfide, tin telluride, lead tin telluride, thallium tin telluride, thallium germanium telluride, bismuth telluride, cadmium phosphide, cadmium arsenide, cadmium antimonide, zinc phosphide, zinc arsenide, zinc antimonide, lead(II) iodide, molybdenum disulfide, gallium selenide, tin sulfide, bismuth sulfide, copper indium gallium selenide, platinum silicide, bismuth(III) iodide, mercury(II) iodide, thallium(I) bromide, titanium dioxide (anatase), copper(I) oxide, copper(II) oxide, uranium dioxide, and uranium trioxide. The partially-conducting slab **102** can be composed of one or more organic semiconductors. The partially-conducting slab **102** and magnetic semiconductors such as magnetite, manganese-doped indium arsenide, manganese-doped gallium arsenide, manganese-doped indium antimonide, manganese- and iron-doped indium oxide, manganese-doped zinc oxide, n-type cobalt-doped zinc oxide, cobalt-doped titanium dioxide, chromium-doped rutile, iron-doped rutile, iron-doped anatase, nickel-doped anatase, manganese-doped tin dioxide, and iron-doped tin dioxide.

The partially-conducting slab **102** can additionally or alternatively be a dielectric loaded with conductive particles, such as ions, silver, gold, copper, aluminum, platinum, iron, carbon black, and alloys thereof. The conductive particles can be introduced into the dielectric in a manner similar to semiconductor doping techniques.

The partially-conducting slab **102** can be a non-conductive material coated with a thin metal film, such as silver, gold, copper, aluminum, platinum, iron, and alloys thereof. The film can be applied with coating techniques such as physical vapor deposition (PVD) or chemical vapor deposition (CVD). It will be appreciated by one of skill in the art that many other methods can be used and that certain methods may be advantageous for particular coatings and/or non-conductive materials.

The thin metal film can be any film thinner than the wavelength of interest. In some embodiments, the thin metal coating is less than about 10 angstroms thick. In some embodiments, the thin metal film can have a resistivity of about $377\Omega/\square$, particularly where the radiation angle of incidence is less than 20° from the normal of the structure. Thin metal films with other resistivities can also be utilized depending on the specifications of the device. For example, the resistivity can be between about $225\Omega/\square$, about $250\Omega/\square$, about $275\Omega/\square$, about $300\Omega/\square$, about $325\Omega/\square$, about $350\Omega/\square$, about $375\Omega/\square$, about $400\Omega/\square$, about $425\Omega/\square$, about $450\Omega/\square$, about $475\Omega/\square$, about $500\Omega/\square$, about $525\Omega/\square$, about $550\Omega/\square$, about $575\Omega/\square$, and the like.

In some embodiments, the partially-conducting slab has a uniform conductivity profile value of about 0.066 Siemens per centimeter (S/cm).

In some embodiments, the modulating reflector disk **104** is composed of a metal. The metal can, in some embodiments, be a highly-conductive metal such as copper, silver, and aluminum.

The partially-conducting slab **102** and the modulating reflector disk **104** can be separated by a gap **108** and can be coupled with one or more mechanical fasteners **110a-d**, such as screws, bolts, nails, rivets, and the like. For example, the fasteners **110a-d** can be bolts or screws coupled with one or more spacers such as washers. One or more of the washers can be selectively removed to adjust the gap **108**. The gap **108** need not be devoid of any material. Rather, the gap **108** can be open to the atmosphere. In other embodiments, the partially-conducting slab **102** and the modulating reflector disk **104** are bonded with a submillimeter wavelength transparent adhesive that functions as a gap **108**.

In other embodiments, the partially-conducting slab **102** and the modulating reflector disk **104** can be free of each other. The modulating reflector disk **104** can be rotated while it is kept parallel to the partially-conducting slab **102**.

The gap **108** can be configured to achieve maximal absorption of incident electro-magnetic radiation at submillimeter wavelengths. In some embodiments (e.g., embodiments in which the gap **G** is air), the gap **G** is defined as

$$G \approx n_g \frac{\lambda}{2} + d_g \frac{\lambda}{2} \quad (4)$$

wherein n_g is a non-negative integer, λ is the wavelength of interest, and $0 \leq d_g \leq 1$. Parameter d_g will vary depending on the properties of the partially-conducting slab **102**. The properties of the partially-conducting slab **102** affecting d_g are the thickness of the slab **102**, the electrical conductivity of the slab **102**, and the electrical permittivity of the slab **102**. For example, if a slab **102** is provided with a uniform electrical conductivity of 0.066 S/cm, thickness of 820 μm , and relative electrical permittivity of 11.9 F/m, and the frequency of interest is 640 GHz ($\lambda=468.75 \mu\text{m}$), the desired gap **G** between the plates for maximal absorption of radiation can be expressed as follows:

$$G \approx n_g \frac{\lambda}{2} + \frac{78}{2} \approx n_g \frac{\lambda}{2} + 0.16 \frac{\lambda}{2}. \quad (5)$$

Parameters n_g and n_m can, but need not necessarily equal each other modulations when the modulations are depressions, but are preferably different when the modulations are bumps. d_g and d_m are preferably different in either case. Parameters n_g

and n_m are preferably as small as possible, particularly where the modulations are depressions.

In other embodiments in which the partially-conducting slab **102** is made of a non-conductive material coated with a thin metal film on the side adjacent to the reflecting disk **104**, the gap **108** can be about one odd multiple of a quarter of a wavelength of the energy to be detected. For example, if the wavelength to be detected is about 2,800 μm , the gap **108** can be about 700 μm (if the modulations are depressions), about 2,100 μm , about 3,500 μm , and so on.

In some embodiments, the modulations **106** are arranged in a single-turn spiral starting from an external radial point of the reflecting disk **104** and proceeding to the center of the disk **104** in a manner similar to a gramophone record. In order to minimize the curvature of scan lines, a large disk **104** can be used with small modulations **106** located closer to the perimeter of the disk. An example of such a disk is depicted in FIG. 1C.

As depicted in FIGS. 2A-H, modulations **206** can be either bumps (**206a**, **206b**, **206c**) or depressions (**206d**, **206e**, **206f**). Modulations **206** can be any shape including a cylinder (**206a**, **206d**), a cuboid (**206b**, **206e**), and right triangular prism (**206c**, **206f**). The shape of modulation **206** may have a diminishing effect on the quality or quantity of reflections as the modulations decrease in size. The face of the modulations **206** are preferably parallel to the face of partially-conductive slab **102** and modulating reflector disk **104**.

The spatially-selective reflective structure **100** provided herein is particularly useful for submillimeter imaging and other imaging techniques where the resolution of existing imagers is constrained either by technology or cost.

Imaging Systems

FIG. 3A depicts a system **300** incorporating a spatially-selective reflective structure **302**. A submillimeter wave source **304** emits radiation at a desired wavelength. Submillimeter wave source **304** exposes object of interest **306** with submillimeter waves, which are reflected to submillimeter optics **308**. Focusing mirror **308** directs the reflection to spatially-selective reflective structure **302**. As spatially-selective reflective structure **302** is spun by motor **310**, modulations **312** are individually brought into the focal plane of focusing mirror **308** and reflect the submillimeter wave to submillimeter receiver **314**.

Submillimeter radiation (also known as “terahertz radiation”, “terahertz waves”, “terahertz light”, “T-rays”, “T-light”, “T-lux”, and “THz”) is generally used to describe the region of the electromagnetic spectrum between about 300 gigahertz (3×10^{11} Hz) and about 3 terahertz (3×10^{12} Hz), which corresponds to wavelength ranges between about 1 millimeter and about 100 micrometers. Submillimeter radiation can be produced by devices such as gyrotrons, backward wave oscillators (BWOs), far infrared lasers (FIR lasers), quantum cascade lasers, free electron lasers (FELs), synchrotron light sources, and photomixing devices.

Gyrotrons are available from Communications & Power Industries of Palo Alto, Calif.; Gyrotron Technology, Inc. of Bensalem, Pa.; Thales Group of Neuilly-sur-Seine, France; and Toshiba Corporation of Tokyo, Japan. Backward wave oscillators are described in U.S. Pat. No. 2,880,355. Far infrared lasers are available from Zaubertek, Inc. of Oviedo, Fla., Laser 2000 GmbH of Munich, Germany, and Coherent, Inc. of Santa Clara, Calif. Quantum cascade lasers are described in U.S. Pat. Nos. 7,359,418 and 7,386,024 and U.S. Patent Application Publication Nos. 2008/0069164 and 2008/0219308. Free electron lasers are described in U.S. Pat. No. 7,342,230. Synchrotron light sources are available from Lyncean Technologies, Inc. of Palo Alto, Calif. Photomixing

devices are described in U.S. Pat. Nos. 7,105,820 and 7,326,930 and U.S. Patent Application Publication Nos. 2005/0156110; 2006/0054824; and 2007/0229937. Integrated submillimeter generators and detectors are available under the PICOMETRIX® T-RAY™ trademark from Advanced Photonix, Inc. of Ann Arbor, Mich.

Submillimeter optics **308** can include one or more focusing mirrors (also known as “concave mirrors”) are available from suppliers such as Edmund Optics Inc. of Barrington, N.J. Focusing minors can composed of glass, metal, or other materials capable of reflecting submillimeter radiation. Suitable minors (e.g. gold-coated aluminum substrates) are available from RadiaBeam Technologies, LLC of Marina Del Ray, Calif.

Motor **310** spins at a speed sufficient to produce a desired number of frames per minute. For example, if the receiver **314** is to capture images at a rate of 30 frames per second, motor **310** can spin spatially-selective reflective structure **302** at a rate of 1,800 revolutions per minute. Motor **310** can, in some embodiments, be a servomechanical device capable of actuation to defined rotational positions and/or capable of self-correction of deviations from a desired rotational position and/or speed.

Imaging Methods

Referring to FIGS. 4A-4C, an image of object **306** (in this example, a knife) is acquired by submillimeter receiver **314** from a spatially-selective reflective structure **302**, e.g. a spatially-selective reflective structure including a modulating reflector disk **104** as depicted in FIG. 1C. Receiver **314** focuses on a viewing window **402** on the spatially-selective reflective structure **302**. Viewing window **402** can be a physical opening in an absorptive material or can be a region that the receiver **314** focuses on while the spatially-selective reflective structure **302** rotates through the viewing window **402**. The absorptive material can be positioned adjacent to the partially-conductive slab **102** or receiver **314** and is preferably positioned as close to the partially-conductive slab as possible. Suitable absorptive materials include ECCOSORB® materials (available from Emerson & Cuming of Randolph, Mass.) and radar absorbent materials (RAM).

As the spatially-selective reflective structure **302** rotates, the modulation **106a** on the outer radius of the spiral enters the viewing window **402**. The energy reflected from the modulation is recorded as the modulation **106a** moves across the window. The recorded data is represented and stored as a function of the modulation position, as depicted as element **404a** in FIGS. 4A-4C. The process continues with modulations **106b**, **106c**, **106d**, **106e**, **106f**, **106g**, **106h** to image rows **404b**, **404c**, **404d**, **404e**, **404f**, **406g**, **404h**, respectively. At this point, modulation **106a** reenters the viewing window **402** and the process is repeated to capture another image.

FIG. 5 depicts an imaging method according to one embodiment of the invention. In step S502, an imaging device is provided, for example an imaging device described herein. The imaging device can include submillimeter wave optics, a spatially-selective reflective structure, a motor configured to rotate the spatially-selective reflective structure, and a submillimeter wave receiver as described herein. In step S504, the motor is actuated to rotate the spatially-selective reflective structure. In step S506, a plurality of reflections are captured by the submillimeter wave receiver. In step S508, each reflection is stored as a pixel. In step S510, an image is formed from a plurality of pixels.

In step S512, the image can be processed with an image recognition method capable of identifying suspicious items that could be a weapon or contraband. Various suitable methods are known to those of skill in the art and include edge

11

detection algorithms and artificial intelligence algorithms (e.g. neural nets) such as those described in U.S. Pat. Nos. 7,310,442 and 7,417,440 and U.S. Patent Application Publication No. 2008/0212742 and in Mohamed-Adel Slamani et al., "Image Processing Tools for the Enhancement of Concealed Weapon Detection," 3 *Proc. Int'l Conf. on Image Processing* 518-22 (October 1999). One or more privacy algorithms can also be applied to the images to obscure sensitive regions such as human genitalia.

In step S514, the image can be stored either by dedicated hardware or software or by a general purpose computer programmed to acquire, store, display, and/or transmit the images.

The images can be stored in variety of formats including known and proprietary vector graphics formats such as vector graphics formats and raster graphics formats. Vector graphics (also called geometric modeling or object-oriented graphics) utilize geometrical primitives such as points, lines, curves, and polygons to represent images. Examples of vector graphics formats include the Scalable Vector Graphics (SVG) and Vector Markup Language (VML) formats. The SVG format is defined at W3C, *Scalable Vector Graphics (SVG)*, <http://www.w3.org/Graphics/SVG/>. VML is described in Brian Matthews, et al., *Vector Markup Language (VML)*, <http://www.w3.org/TR/1998/NOTE-VML-19980513>. Alternatively, the images can be converted to or maintained in a raster graphics format, which is a representation of images as a collection of pixels. Examples of raster graphics formats include JPEG, TIFF, RAW, PNG, GIF, and BMP.

The images can also be compiled into a video format such as BETAMAX®, BLU-RAY DISC®, DVD, D-VHS, Enhanced Versatile Disc (EVD), HD-DVD, Laserdisc, M-JPEG, MPEG-1, MPEG-2, MPEG-4, Ogg-Theora, VC-1, VHS, and the like.

Image and/or video files can be stored on media such as magnetic media (e.g. tapes, discs), optical media (e.g. CD-ROM, CD-R, CD-RW, DVD, HD DVD, BLU-RAY DISC®, Laserdisc), punch cards, and the like. Image and/or video files can also be transmitted to a remote storage device by a variety of standards such as parallel or serial ports, Universal Serial Bus (USB), USB 2.0, Firewire, Ethernet, Gigabit Ethernet, and the like.

In step S516, the images or video can be displayed on a display device such as a cathode ray tube (CRT), a plasma display, a liquid crystal display (LCD), an organic light-emitting diode display (OLED), a light-emitting diode (LED) display, an electroluminescent display (ELD), a surface-conduction electron-emitter display (SED), a field emission display (FED), a nano-emissive display (NED), an electrophoretic display, a bichromal ball display, an interferometric modulator display, a bistable nematic liquid crystal display, and the like.

In step S518, images can also be printed with devices such as laser printers, ink jet printers, dot matrix printers and the like.

As one will appreciate, the steps of the methods described herein can be configured to place various steps in various orders and may include additional steps or omit steps listed in FIG. 5. Specifically, one of skill in the art will realize that image handling steps S512, S514, S516, and S518 can be practiced various orders and/or combinations.

Optimization of Spatially-Selective Reflective Structures

Referring now to FIG. 6, the reflectivity of a spatially reflective structure can be represented with a three layer model 600. Radiation from source 602 (e.g. reflections from an object of interest), passes through the air (E1), partially-conducting slab (E2), and gap (E3), before reflecting off the modulating reflector disk 104 before passing through partially-conducting slab (E2) and air (E1) and being imaged by imager 604. The electric field for each layer (E1, E2, E3) can be expressed in the following matrices, where E_i^{\pm} is the

12

electric field in the i^{th} layer and the plus or minus sign indicates the direction of propagation as depicted in FIG. 6:

$$\begin{bmatrix} e^{j\gamma_1 z_1} & -e^{-j\gamma_2 z_1} & -e^{j\gamma_2 z_1} & 0 & 0 \\ \frac{e^{j\gamma_1 z_1}}{\eta_1} & -\frac{e^{-j\gamma_2 z_1}}{\eta_2} & \frac{e^{j\gamma_2 z_1}}{\eta_2} & 0 & 0 \\ 0 & e^{-j\gamma_2 z_2} & e^{j\gamma_2 z_2} & -e^{-j\gamma_3 z_2} & -e^{-j\gamma_3 z_2} \\ 0 & \frac{e^{-j\gamma_2 z_2}}{\eta_2} & -\frac{e^{j\gamma_2 z_2}}{\eta_2} & \frac{e^{-j\gamma_3 z_2}}{\eta_3} & \frac{e^{j\gamma_3 z_2}}{\eta_3} \\ 0 & 0 & 0 & e^{-j\gamma_3 z_3} & e^{j\gamma_3 z_3} \end{bmatrix} \begin{bmatrix} E_1^- \\ E_2^+ \\ E_2^- \\ E_3^+ \\ E_3^- \end{bmatrix} = \begin{bmatrix} -E_1^+ e^{-j\gamma_1 z_1} \\ \frac{E_1^+}{\eta_1} e^{-j\gamma_1 z_1} \\ 0 \\ 0 \\ 0 \end{bmatrix} \quad (6)$$

The variable z_i is the thickness of the layer.

The complex propagation constants for each layer are given by the formula $\gamma_i = \alpha_i + j\beta_i$ with

$$\alpha_i = \omega \left\{ \frac{\mu_i \epsilon_i'}{2} \left[\sqrt{1 + \frac{\epsilon_i''}{\epsilon_i'}} - 1 \right] \right\}^2 \quad (7a)$$

and

$$\beta_i = \omega \left\{ \frac{\mu_i \epsilon_i'}{2} \left[\sqrt{1 + \frac{\epsilon_i''}{\epsilon_i'}} + 1 \right] \right\}^2 \quad (7b)$$

The impedance for each layer is given by

$$\eta_i = \sqrt{\frac{\mu_i}{\epsilon_i'}} \left(1 - j \frac{\epsilon_i''}{\epsilon_i'} \right)^{-\frac{1}{2}} \quad (8)$$

In equations (7) and (8), $\epsilon_i' = \epsilon_i$ (the dielectric permittivity of layer i) and

$$\epsilon_i'' = \frac{\sigma_i}{\omega}$$

where σ_i is the conductivity of the layer. The radial frequency is given by $\omega = 2\pi f$ where f is the frequency of the terahertz field. The layers are assumed to be non-magnetic, so that $\mu_i = \mu_0$, which is the magnetic permeability of free space.

Matrix equation (6) can be easily solved with the help of numerical computing software such as MATLAB®, available from The MathWorks of Natick, Mass., MAPLE®, available from Waterloo Maple, Inc. of Waterloo, Ontario, and the like. The reflection coefficient Γ can be obtained from the ratio

$$\Gamma = \left| \frac{E_1^-}{E_1^+} \right|$$

FIG. 6B depicts reflection coefficient Γ as a function of gap distance (i.e. $z_3 - z_2$), partially-conductive slab thickness (i.e. $z_2 - z_1$), and partially-conductive slab conductivity. FIG. 6B(i)

13

depicts reflection coefficient Γ as a function of reflector distance for a slab with conductivity 0.066 S/cm and thickness 820 μm . FIG. 6B(ii) depicts reflection coefficient Γ as a function of slab thickness for a slab with conductivity 0.066 S/cm and reflector distance of 1440 μm . FIG. 6B(iii) depicts reflection coefficient Γ as a function of slab conductivity for a slab of thickness 820 μm and reflector distance of 1440 μm .

As discussed herein, modulation height is preferably selected for maximal reflection of radiation while gap G is preferably selected for maximal absorption of radiation. These values can be identified by selecting a local maxima in FIG. 6B(i) for the modulation height or depth and selecting a local minima in FIG. 6B(i) for the gap value. In generally, optimal modulation heights approximate multiples of one-half of the wavelength of energy to be detected.

Further Reflector Disks

Referring now to FIG. 7, another embodiment of a modulating reflector disk 704 is depicted. Modulating reflector disk 704 includes a plurality of modulations 706 that are arranged in such a manner that as the disk 704 is rotated the orientation of modulations 706 produces a matrix having linearly independent rows as discussed herein, thus ensuring that the inverse of the matrix exists. Although random placement of pixels will almost always produce such an arrangement, the arrangement of modulations can be produced by a human or by a computer algorithm.

In order to utilize modulating reflector disk 704, receiver 314 focuses on a viewing window 702 as discussed above in the context of FIGS. 3 and 4 herein. However, instead of defining viewing window 702 to encompass a single modulation at any given time as in FIG. 4, viewing window 702 can encompass a plurality of modulations 706.

In order to permit a low resolution receiver 314 (e.g., a single-pixel imager such as a submillimeter antenna) to capture multi-pixel images, viewing window 702 is divided into a plurality of arbitrary, non-physical pixels 708.

FIG. 8 depicts an exaggerated disk 804 and a viewing window 802 having nine pixels p_1 - p_9 in order to depict an imaging method 900 described in FIG. 9. In step S902, an imaging device is provided (e.g., an imaging device as described herein). As the disk 804 is rotated (S904), receiver 314 takes a number of measurements equal to the number of arbitrary pixels in viewing window 802 (S906). For example, in the nine-pixel embodiment depicted in FIG. 8, receiver 314 can take a measurement at 40° increments of rotation of disk 804.

Measurements need not occur at regular intervals and need not encompass a complete revolution of disk 804. For example, in the nine-pixel embodiment depicted in FIG. 8, receiver 314 can take measurements at 10° increments of rotation of disk 804 to obtain four 3×3 images. In such an embodiment, measurements at 0°, 10°, 20°, 30°, 40°, 50°, 60°, 70°, and 80° are used to produce a first image; measurements at 90°, 100°, 110°, 120°, 130°, 140°, 150°, 160°, and 170° are used to produce a second image; measurements at 180°, 190°, 200°, 210°, 220°, 230°, 240°, 250°, and 260° are used to produce a third image; and measurements at 270°, 280°, 290°, 300°, 310°, 320°, 330°, 340°, and 350° are used to produce a fourth image.

The measurements used to generate consecutive images can overlap. For example, if one seeks to obtain a plurality of 18×18 pixel images, 324 measurements are required for each image. If measurements are obtained at 1° increments, the first image can be obtained from measurements from 0° to 323°, the second image can be obtained from measurements from 324° of the first revolution to 286° of the second revolution, and so on.

14

Although it is possible to obtain series of images that are each captured at a unique set of rotational positions, it may be preferable in some embodiments to capture each image at the same set of rotational positions (e.g., 1° increments from 0° to 323° on each revolution) in order to minimize processing and storage requirements by only storing a single, pre-calculated measurement matrix (see equation 10) and its inverse (see equation 11).

In order to produce a multi-pixel image, the fraction of the each pixel area that is backed by a modulation is calculated for each rotational position at which a measurement will be taken. For example, at the rotational position depicted in FIG. 8, 40% of pixel p_1 , 15% of pixel p_2 , 55% of pixel p_3 , 22% of pixel p_4 , 20% of pixel p_5 , 8% of pixel p_6 , 43% of pixel p_7 , 36% of pixel p_8 , and 70% of pixel p_9 are backed by one or more modulations. At this first position, a measurement m_1 is taken. This measurement m_1 will reflect the signal reflected onto receiver 314 by the portion of viewing window 802 that is backed by modulations as reflected in equation (9) below.

$$m_1 = 0.4p_1 + 0.15p_2 + 0.55p_3 + 0.22p_4 + 0.2p_5 + 0.08p_6 + 0.43p_7 + 0.36p_8 + 0.7p_9 \quad (9)$$

This equation can be solved as part of a system of linear equations along with the equations obtained at other rotational positions (S908). These equations can be expressed in matrix form as shown in equation (10) below wherein dots (.) represent the coefficients in front of pixels p_1 - p_9 for the other positions of the disk 804 and m_1 - m_9 represent the corresponding measured signal for each position. As will be appreciated by one of skill in the art, the rows of the matrix are preferably independent of each other, so that the system of linear equations can be solved.

The 9×9 matrix in equation (10) is the measurement matrix mentioned previously. For an image with n pixels, the measurement matrix will have dimensions of $n \times n$.

$$\begin{bmatrix} 0.4 & 0.15 & 0.55 & 0.22 & 0.2 & 0.08 & 0.43 & 0.36 & 0.7 \\ \vdots & \vdots & \vdots & \vdots & \vdots & \vdots & \vdots & \vdots & \vdots \\ \vdots & \vdots & \vdots & \vdots & \vdots & \vdots & \vdots & \vdots & \vdots \\ \vdots & \vdots & \vdots & \vdots & \vdots & \vdots & \vdots & \vdots & \vdots \\ \vdots & \vdots & \vdots & \vdots & \vdots & \vdots & \vdots & \vdots & \vdots \\ \vdots & \vdots & \vdots & \vdots & \vdots & \vdots & \vdots & \vdots & \vdots \\ \vdots & \vdots & \vdots & \vdots & \vdots & \vdots & \vdots & \vdots & \vdots \\ \vdots & \vdots & \vdots & \vdots & \vdots & \vdots & \vdots & \vdots & \vdots \\ \vdots & \vdots & \vdots & \vdots & \vdots & \vdots & \vdots & \vdots & \vdots \end{bmatrix} \times \begin{bmatrix} p_1 \\ p_2 \\ p_3 \\ p_4 \\ p_5 \\ p_6 \\ p_7 \\ p_8 \\ p_9 \end{bmatrix} = \begin{bmatrix} m_1 \\ m_2 \\ m_3 \\ m_4 \\ m_5 \\ m_6 \\ m_7 \\ m_8 \\ m_9 \end{bmatrix} \quad (10)$$

The matrix equation can be solved for values p_1 - p_9 as shown in equation (11) below:

15

$$\begin{bmatrix} p_1 \\ p_2 \\ p_3 \\ p_4 \\ p_5 \\ p_6 \\ p_7 \\ p_8 \\ p_9 \end{bmatrix} = \quad (11)$$

$$\begin{bmatrix} 0.4 & 0.15 & 0.55 & 0.22 & 0.2 & 0.08 & 0.43 & 0.36 & 0.7 \\ \vdots & \vdots & \vdots & \vdots & \vdots & \vdots & \vdots & \vdots & \vdots \\ \vdots & \vdots & \vdots & \vdots & \vdots & \vdots & \vdots & \vdots & \vdots \\ \vdots & \vdots & \vdots & \vdots & \vdots & \vdots & \vdots & \vdots & \vdots \\ \vdots & \vdots & \vdots & \vdots & \vdots & \vdots & \vdots & \vdots & \vdots \\ \vdots & \vdots & \vdots & \vdots & \vdots & \vdots & \vdots & \vdots & \vdots \\ \vdots & \vdots & \vdots & \vdots & \vdots & \vdots & \vdots & \vdots & \vdots \\ \vdots & \vdots & \vdots & \vdots & \vdots & \vdots & \vdots & \vdots & \vdots \\ \vdots & \vdots & \vdots & \vdots & \vdots & \vdots & \vdots & \vdots & \vdots \end{bmatrix}^{-1} \times \begin{bmatrix} m_1 \\ m_2 \\ m_3 \\ m_4 \\ m_5 \\ m_6 \\ m_7 \\ m_8 \\ m_9 \end{bmatrix}$$

The values p_1 - p_9 can be used to generate a multi-pixel image (S910). For example, values p_1 - p_9 can be mapped to grayscale values to produce a grayscale image. Alternatively, values p_1 - p_9 can be mapped to black or white to produce a black-and-white image.

The image can then be processed (S912), stored (S914), displayed (S916), and/or printed (S918) as discussed herein.

As will be appreciated by one of skill in the art, the systems and methods described herein can be scaled to produce images larger than the examples described herein. For example, to produce a 100×100 pixel image, 10,000 measurements are obtained (corresponding to 10,000 distinct modulation patterns). These measurements can be obtained by taking a measurement every 0.036° (360°/10000).

Additional Imaging Systems

In some embodiments of the invention, an imaging system (e.g., the imaging system described in the context of FIG. 3A herein) is configured to prevent radiation reflected by the object of interest 306 from directly entering receiver 314. A variety of approaches can be utilized to achieve this goal.

In one embodiment, the receiver 314 includes a highly-directive antenna directed toward the imaging window on the spatially selective mirror so that energy received directly from the object of interest 306 is severely attenuated.

In another embodiment depicted in FIG. 3B, a blocking mask of radar-absorbing material (RAM) 316 can be placed around the receiver 314 to prevent external radiation from reaching the receiver 314.

In still another embodiment depicted in FIG. 3C, a beam splitter 318 allows for the positioning of receiver 314 away from the likely path of ambient energy reflected by object of interest 306.

In some embodiments, the imaging system is designed for “standoff” detection, for example, from a distance of about 5 to 50 meters from an object of interest. However, embodiments of the invention herein can be configured to scan objects of interest at ranges of less than 5 meters or greater than 50 meters from an object of interest. For example, as depicted in FIG. 3D, an imaging system can include one or more secondary optics 318a, 318b (e.g., optics having

16

aplanatic surfaces). The secondary optics 318 can be movable in order to focus the imaging system 300d.

Optimization of Partially-Conducting Slabs

As discussed herein and depicted in FIG. 10, in some embodiments, partially-conducting slab 1002 can be a non-conductive material 1012 coated with a thin metallic film 1014. This embodiment of the partially-conducting slab 1002 is also referred to herein as a “resistive sheet.”

The optimal parameters for the distance of the modulations and the resistive sheet 1002 can be expressed by the formula in the context of FIGS. 11A-11C:

$$d_n = n \frac{\lambda}{2\sqrt{\epsilon_r \cos(\phi_i)}}, \quad (12)$$

$$n = 1, 2, \dots$$

where ϵ_r is the relative permittivity of the media between the thin metallic layer 1014 and the modulation 1006, λ is the wavelength of interest, and ϕ_i is the angle of radiation incidence given with respect to the normal of the spatially-selective mirror 1000.

Similarly, the optimal distance for absorption (i.e., the distance between the metallic layer 1014 and the area of reflector disk 1004 without a modulation 1006) can be expressed by the formula:

$$d_r = \frac{(2n-1)\lambda}{4\sqrt{\epsilon_r \cos(\phi_i)}}, \quad (13)$$

$$n = 1, 2, \dots$$

The optimal value of the resistivity depends on the angle of incidence ϕ_i . FIGS. 12A-12I depict the results of a method of moments analysis to calculation the reflectivity of a structure similar to the structure depicted in FIG. 11C.

FIGS. 12A-12C depict the power reflectivity coefficient as a function of reflector distance and/or sheet resistivity for radiation normally incident to the structure. FIG. 12A depicts the \log_{10} of the reflectivity as a function of reflector distance (x-axis) and the sheet resistivity (y-axis). FIGS. 12B and 12C depict slices through the lines in FIG. 12A, but are displayed linearly (i.e., not in \log_{10}).

FIGS. 12D-12F depict the power reflectivity coefficient as a function of reflector distance and/or sheet resistivity for radiation incident to the structure at 10° off the normal. FIG. 12D depicts the \log_{10} of the reflectivity as a function of reflector distance (x-axis) and the sheet resistivity (y-axis). FIGS. 12E and 12F depict slices through the lines in FIG. 12D, but are displayed linearly (i.e., not in \log_{10}).

FIGS. 12G-12I depict the power reflectivity coefficient as a function of reflector distance and/or sheet resistivity for radiation incident to the structure at 20° off the normal. FIG. 12G depicts the \log_{10} of the reflectivity as a function of reflector distance (x-axis) and the sheet resistivity (y-axis). FIGS. 12H and 12I depict slices through the lines in FIG. 12G, but are displayed linearly (i.e., not in \log_{10}).

As depicted in FIGS. 12A-12I, the optimal parameters change with the angle of incidence. The distance parameters as a function of radiation incidence angle are given by equations (12) and (13) and sheet resistivity can be maintained at approximately that of free space (i.e., about 377Ω/□) for angles of incidence less than about 20°.

17

Additionally, as depicted in FIGS. 12A-12I, the dynamic range of the reflector (minimum to maximum reflectivity range) is larger if the radiation is normally incident on the structure. In this regard, embodiments of the imaging systems including a beam splitter 318 such as depicted in FIG. 3C may be preferred in certain situations over the configuration depicted in FIG. 3A.

As discussed herein, depressions can be preferred over modulations in some embodiments of the invention. In general, spatially-selective reflector structures having depressions perform better, particularly when the gap between the thin metallic film and the absorbing portion of the reflector disk is minimized.

In some embodiments, the linear dimension (i.e., width or diameter) of the modulation is at least three wavelengths of interest. Increasing the dimension of the non-uniformity can increase the level of the reflected signal. However, if the modulation scheme of the spatially selective mirror is raster scanning, increasing the dimension of the non-uniformity can increase the blur in the detected image. Accordingly, in some embodiments, the proper linear dimension for the non-uniformity in this case is greater than three wavelengths and less than $\lambda F\#$, where $F\#$ is the F-number of the optics of the system and) is the radiation wavelength of interest.

FIGS. 13A and 13B depict the power reflection profile of a spatially-selective reflective structure having a depression of linear dimensions 2λ and 3λ , respectively, for a reflective structure wherein the depression distance and reflector distance from the resistive sheet are

$$\frac{\lambda}{2} \text{ and } \frac{\lambda}{4},$$

respectively, the sheet resistivity is $377\Omega/\square$, and the radiation is normally incident to the structure. As depicted by the plots in FIGS. 13A and 13B, the reflection profile of the 3λ depression (i.e., FIG. 13B) is more effective than the 2λ depression (i.e., FIG. 13A). The maximum value of the reflection coefficient was 1 for the 3λ depression and about 0.97 for the 2λ depression. Furthermore, the reflection profile for the 3λ depression was more defined than that of the 2λ depression, i.e., the reflection profile have a wider constant reflection profile.

FIGS. 14A and 14B depict the power reflection profile of a spatially-selective reflective structure having a bump distance and reflector distance of

$$\frac{\lambda}{2} \text{ and } \frac{3\lambda}{4},$$

respectively, a sheet resistivity of $377\Omega/\square$, and radiation normally incident to the structure.

As depicted in FIGS. 13A-14B, portions of the reflection profiles oscillate around zero. Negative values exist because the reflection coefficient is calculated by subtracting the absorption coefficient (i.e., the physical quantity that is calculated from the currents on the resistive sheet) from 1. These oscillations are caused by diffraction of the electric field by the edges of the non-uniformities and become more evident as the distance between the reflector and the resistive sheet increases or if the modulations are bumps. These diffracted fields interfere with the fields that are incident on the resistive sheet and the fields that are reflected from the reflector to cause the undulations depicted in FIGS. 13A-14B.

18

FIG. 15 depicts the power reflection coefficient for a structure that is modulated by two depressions separated by a gap that varies from 0.1λ to 10λ . The depression distance and reflector distance from the resistive sheet were

$$\frac{\lambda}{2} \text{ and } \frac{\lambda}{4},$$

respectively; the sheet resistivity was $377\Omega/\square$; and the radiation was normally incident to the structure.

Each column of the plot is one reflectivity profile corresponding to a separation as indicated on the x-axis. The plot shows that when the distance between the depressions (i.e., the separation distance as depicted on the x-axis of FIG. 15) is greater than 5λ and every subsequent multiple of a wavelength, the undulations in the region between depressions are minimized. Also, the undulations on the outsides of the depressions are minimized when the separation is an odd multiple of the wavelength that is greater than or equal to 5λ (e.g., 5λ , 7λ , 9λ , and so on). Furthermore, the undulations almost disappear when the distance between the depressions is greater than 10λ .

Inter-modulation distances need not be a multiple of the wavelength of interest. For example, undulations are acceptably low when the inter-modulation distance is a non-event multiple of a wavelength (e.g., 3.6λ , 4.4λ , 6.7λ , and so on).

FIGS. 16A, 16B, 16C, and 16D depict slices of FIG. 15 and provide reflectivity profiles for separations of 4λ , 4.5λ , 5λ , and 10λ , respectively.

Accordingly, in some embodiments of the invention, modulations are separated by a multiple of a wavelength of interest λ . For example modulations can be separated by about 1λ , about 2λ , about 3λ , about 4λ , about 5λ , about 6λ , about 7λ , about 8λ , about 9λ , about 10λ , about 11λ , about 12λ , about 13λ , about 14λ , about 15λ , about 16λ , about 17λ , and the like.

As will be appreciated by one of ordinary skill in the art, absorption profiles can be generated for any potential reflective structure using existing software programs. Such modeling can be desirable both to calculate the matrices discussed herein as well as to optimize the performance of the reflective structure.

Reflector Disks and Methods of Fabricating the Same

Referring now to FIG. 17 in the context of FIG. 18, a method 1700 of fabricating a reflector disk is provided.

In step S1702, a metallic disk 1802 is provided. As discussed herein, the metallic disk 1802 can, in some embodiments, be fabricated from a highly-conductive metal such as copper, silver, aluminum, and the like.

In step S1704, one or more modulations 1804 (e.g., bumps or depressions) are formed in the metallic disk 1802. Modulations 1804 can be formed with a variety of techniques including machining, etching, and the like. Alternatively, a metallic disk 1802 can be cast or molded with modulations 1804. Modulations 1804 can, in some embodiments, be dimensioned according to the principles and equations discussed herein.

In step S1706, a dielectric layer 1806 is applied to the metallic disk 1802. The dielectric layer 1806 is preferably transparent to the frequency of interest. Suitable dielectric materials include, for example, polyethylene terephthalate (PET) (available under the MYLAR® trademark from E. I. Du Pont de Nemours and Company of Wilmington, Del.) and the like.

19

In step S1708, the dielectric material **1806** can be machined to produce a uniform thickness. In some embodiments, the dielectric material has a thickness as discussed herein.

In step S1710, a metallic film **1808** can be deposited on the dielectric material **1806** as discussed herein. The metallic film **1808** can be a metal, for example a highly-conductive metal such as aluminum, copper, silver, gold, and the like. The thickness of the metallic film **1808** can, in some embodiments, be such that the resistivity of the film **1808** is equal to that of free space (i.e., approximately $377\Omega/\square$).

Motors and Viewing Windows

Referring now to FIG. 19A, a spatially-selective reflector device and motor assembly **1900a** is provided. A motor **1910** spins a spatially-selective reflector structure **1902a** (e.g., a spatially-selective reflector structure as described herein) behind a shield **1904a** defining a viewing window **1906a**. In some embodiments, the shield **1904a** is coated with or fabricated from an absorptive material such as ECCOSORB® materials (available from Emerson & Cuming of Randolph, Mass.) and radar absorbent materials (RAM).

Structure **1902a** can be rotated continuously and at a constant speed by a spindle motor such as those used in hard disk drives. If the structure **1902a** is rotated at a constant speed, the measurement precision is limited only by the integration time of the receiver and the noise level of the receiver system. For example, the bandwidth of the receiver increases as the rate of data acquisition increases but an increase in receiver bandwidth increases the received noise. For an imager of 100 by 100 pixels that forms 30 frames per second, 300,000 measurements are required (corresponding to a receiver bandwidth of 300 KHz).

If the structure **1902a** is rotated at a constant speed, the receiver can be triggered to start sampling the input by a sensor that detects the start of one revolution. This removes the need to have an encoder that can measure $1/10,000^{\text{th}}$ of a rotation. If the receiver samples 10,000 samples per revolution triggered by the revolution sensor then each signal sample corresponds to $1/10,000^{\text{th}}$ of a rotation and each measurement is automatically registered with a rotational position.

In some embodiments, the diameter of the structure **1902a** is between about 2.5 to about 3 times the linear vertical dimension of the imaging window **1906a**.

The size of the imaging window **1906a** can be a function of the desired resolution. For example, to produce an image of 100×100 pixel, wherein each pixel has a 1 mm×1 mm dimension, the imaging window **1906a** will be about 10 cm×10 cm. The structure **1902a** can have a diameter between about 25 cm and about 30 cm. If the pixel linear size is decreased or increased by a ratio R while the number of pixels is held constant, the diameter of structure **1902a** will decrease or increase by the same ratio R.

In some situations, the multi-modulation embodiments of the devices herein may be preferred over a raster scanning embodiments (i.e., embodiments where a single modulation is within the imaging window **1806** at any given time) because (i) the signal received by the receiver is higher (thereby increasing the signal to noise ratio) and (ii) a smaller structure can be utilized. However, in situations in which computing power is limited, a raster scanning embodiment may be preferred.

Without being bound by theory, experimentation has shown that at any give time, about 20% to about 30% of the imaging window can be "covered" by modulations. This percentage can extend beyond this range so long as the conditions discussed herein are satisfied.

20

As depicted in FIG. 19B, a spatially-selective reflector device and motor assembly **1900b** can be provided for a raster scanning embodiment. Instead of a "large" imaging window **1906a** as in the multiple-modulation assembly **1900a**, shield **1904b** includes an imaging window encompassing a single modulation. Shield **1904b** can be moved with respect the diameter of structure **1902b** to generate a 2D image from reflections captured from other modulations (not depicted in FIG. 19B). In other embodiments, structure **1902b** has a single modulation and a 1D image is generated.

Calculation of Measurement Matrix

Referring to FIG. 20, the measurement matrix described herein can be calculated according to method **2000**.

In step S2002, the imaging window is divided into a desired number of pixels.

In step S2004, for a first rotational position of the structure, the centers of modulations visible through the imaging window are calculated.

In step S2006, the area of intercept between the pixel and a modulation is calculated. In some embodiments, the area of intercept can be calculated using a Monte Carlo algorithm or other similar method. For example, if an arbitrary number of points are randomly chosen within each pixel each point will contribute the local reflection coefficient for that point (e.g. 1.0, 0.5, and the like) to the integration.

In step S2008, a row of the measure matrix is formed based on the area of intercept calculated as discussed herein for each pixel in step S2006.

In step S2010, steps S2004-S2008 are repeated for each subsequent pattern of non-uniformities.

As discussed herein, method **2000** need to only be performed once for a given disk and a given pixel division in an imaging window. Therefore, it can be computed to the highest accuracy possible using all available time and computing resources. As discussed herein, it may be preferable in some embodiments to perform a three-dimensional electromagnetic analysis of the entire structure to determine accurately the absorption/reflection profile of the disk so that the measurement matrix is calculated accurately.

Once the measurement matrix is computed, its inverse is computed. Again, this operation only needs to be done once.

The system of linear equations can be solved simply by multiplying the inverse of the measurement matrix by the measurement data. This calculation can be performed by hardware and/or software capable of multiplying a matrix and a vector. For example, this multiplication can be performed by one or more field programmable gate arrays (FPGAs) available from Altera Corporation of San Jose, Calif.

Scanning Applications

As discussed herein, embodiments of the invention can be utilized for standoff scanning (e.g., at large gatherings such as sporting events, parades, rallies, and the like.)

Other embodiments of the invention can be utilized for profiling sensors that scan a single line of a moving object and form an image in time. Such an embodiment can be deployed in environment such as airports, office buildings, and the like where individuals are asked to move through portal. Advantageously, profiling scanners only require the imaging of a single line at any given moment. (The lines are then combined to form an image.) Thus, the reflector size and computation power for image acquisition can be minimized Both multiple-modulation and raster scanning embodiments described herein can be used in profiling scanners.

Referring now to FIG. 21, a profiling scanner **2100** incorporating the imaging devices described herein is provided. An individual **2102** enters the scanner **2100** at a proximal end **2104** and exits at a distal end **2106**. The individual can move

21

through the scanner **2100** by walking or can stand on an optional moving walkway **2108**. As the individual moves through the scanner **2100**, one or more imaging devices **2110a**, **2110b** images a plurality of lines (e.g., substantially horizontal lines) of the individual's body.

In some embodiments one or more optics **2112a**, **2112b** are used to focus the imager. For example, the optics can **2112a**, **2112b** can focus on the floor of the distal end **2106** and proximal end **2104**, respectively. As the individual **2102** moves through the scanner, the individuals entire body will be imaged without the need to adjust the optics **2112**.

EQUIVALENTS

The functions of several elements may, in alternative embodiments, be carried out by fewer elements, or a single element. Similarly, in some embodiments, any functional element may perform fewer, or different, operations than those described with respect to the illustrated embodiment. Also, functional elements (e.g., modules, databases, computers, clients, servers and the like) shown as distinct for purposes of illustration may be incorporated within other functional elements, separated in different hardware, or distributed in a particular implementation.

While certain embodiments according to the invention have been described, the invention is not limited to just the described embodiments. Various changes and/or modifications can be made to any of the described embodiments without departing from the spirit or scope of the invention. Also, various combinations of elements, steps, features, and/or aspects of the described embodiments are possible and contemplated even if such combinations are not expressly identified herein.

INCORPORATION BY REFERENCE

The entire contents of all patents, published patent applications, and other references cited herein are hereby expressly incorporated herein in their entireties by reference.

22

The invention claimed is:

1. A method of submillimeter imaging, the method comprising:

providing:

- submillimeter wave optics;
- a spatially-selective reflective structure located in the focal plane of the submillimeter wave optics;
- a submillimeter wave receiver positioned to capture waves reflected from the spatially-selective reflective structure; and
- a motor configured to rotate the spatially-selective reflective structure;
- actuating the motor to rotate the spatially-selective reflective structure;
- capturing a plurality of reflections from the plurality of modulations as the spatially-selective reflective structure rotates;
- solving a system of equations wherein a magnitude of one of the plurality of reflections is equal to a sum of a product of the reflection in each of a plurality of pixels and the fraction of pixel area backed by the plurality of modulations; and
- forming an image from the plurality of the pixels.

2. The method of claim **1**, wherein the number of equations in the system of equations is equal to the number reflections captured.

3. The method of claim **2**, wherein the plurality of modulations are arranged such that a matrix having a plurality rows, each with elements corresponding to a fraction of each pixel in a viewing window projected onto the disk that is backed by a modulation at a distinct rotational position of the disk, has linearly independent rows.

* * * * *